Three-Way Catalytic Converter Modeling as a Modern Engineering Design Tool

G. N. Pontikakis

G. S. Konstantas

A. M. Stamatelos[1]

e-mail: stam@uth.gr

Mechanical and Industrial Engineering Department,
University of Thessaly,
383 34 Volos, Greece

The competition to deliver ultra low emitting vehicles at a reasonable cost is driving the automotive industry to invest significant manpower and test lab resources in the design optimization of increasingly complex exhaust aftertreatment systems. Optimization can no longer be based on traditional approaches, which are intensive in hardware use and lab testing. This paper discusses the extents and limitations of applicability of state-of-the-art mathematical models of catalytic converter performance. In-house software from the authors' lab, already in use during the last decade in design optimization studies, updated with recent, important model improvements, is employed as a reference in this discussion. Emphasis is on the engineering methodology of the computational tools and their application, which covers quality assurance of input data, advanced parameter estimation procedures, and a suggested performance measure that drives the parameter estimation code to optimum results and also allows a less subjective assessment of model prediction accuracy. Extensive comparisons between measured and computed instantaneous emissions over full cycles are presented, aiming to give a good picture of the capabilities of state of the art engineering models of automotive catalytic converter systems.
[DOI: 10.1115/1.1787506]

Introduction

The catalytic converter has been in use for the past 30 years as an efficient and economic solution for the reduction of pollutants emitted by the internal combustion engine, the latter being the powertrain for almost all vehicles in use today. The widespread use of the catalytic converter was the response of the automotive industry to the legislation of developed countries, which poses limits to the most important gaseous pollutants emitted by both gasoline and diesel engines.

Since the concern about the environmental impact of the emissions of the vehicles fleet is steadily growing—especially in urban areas, where air pollution has become a major issue—emission legislation becomes gradually stricter. Accordingly, this has led to continuous efforts of the automotive industry to improve the efficiency of the catalytic converter [1]. Today's emission standards have been lowered so much that the catalytic converter technology has been pushed to its limits and it became apparent that, in order to build vehicles that comply with the legislation, automotive engineers should tune the whole system of engine, piping, and catalytic converter [2]. Thus there emerged the need to view the catalytic converter as a component of an integrated *exhaust aftertreatment system* that should be designed very accurately.

In this context, the role of modeling of the components of exhaust aftertreatment systems is becoming increasingly important, especially as regards the catalytic converter, which is the most crucial device of such systems. Since the introduction of catalytic converters in production vehicles, catalytic converter models have been appearing in the literature in parallel with the development of new catalytic converter technologies. Nevertheless, the accuracy, reliability, and application range of catalytic converter models is still questioned. The number of modeling applications in the automotive industry remains limited, especially when contrasted to the plethora of models that appear in the literature [3–15]. It seems that a complicated landscape of approaches and methodologies has been created, causing an uncertainty as regards their validity and applicability. Most probably, this adversely affects their application in everyday practice, although modern modeling methodologies have been greatly improved and, in many cases, they have been successfully incorporated in the process of exhaust aftertreatment systems design [16–20].

In what follows, we attempt to inverse this situation, first by sketching an overview of modeling approaches that could help the navigation through the complicated landscape of this field of research. Subsequently, we present our choice of modeling approaches along with some supporting tools, in order to compile a complete methodology that provides the required high accuracy levels for the current state-of-the-art exhaust aftertreatment systems design. This methodology combines a significantly updated version of the CATRAN [21] modeling code with optimization tools tailored to the computer-aided estimation of the model's chemical kinetics parameters. The first steps of the developed optimization methodology have already been presented elsewhere [22]. Here we update and enhance it by incorporating recent improvements of the catalytic converter model and better integration with the supporting tools.

Navigation in the Modeling Landscape

A great number of models have been presented until today, featuring a multitude of approaches and levels of modeling detail. The diversity of published works on the field indicates that no definite answers have been given to the catalytic converter modeling problem [23]. There are several reasons for this situation:

• *Modeling objectives and application range*. Not all published works share common objectives and application range, varying from fast, approximate models to very detailed, computationally intensive models. Fundamental research models formulation usually attempts to describe phenomena as accurately as possible, require a lot of input data and usually can be tested only in extremely simplified catalyst behavior scenarios. For application-oriented models, formulation depends on the system or device where modeling is applied as well as the design parameters under investigation. In this case, accuracy may be sacrificed because of constraints such as simplicity or flexibility.

[1]Author to whom correspondence should be addressed.

Contributed by the Internal Combustion Engine Division of THE AMERICAN SOCIETY OF MECHANICAL ENGINEERS for publication in the ASME JOURNAL OF ENGINEERING FOR GAS TURBINES AND POWER. Manuscript received by the ICE Division, December 1, 2002; final revision received September 1, 2003. Associate Editor: D. Assanis.

• *Problem complexity*. Catalytic converter operation involves heterogeneous catalytic chemical reactions, which are coupled with simultaneous heat and mass transfer and take place under highly transient conditions. Under such conditions, it is difficult to describe chemical phenomena quantitatively or even qualitatively Each set of inevitable approximations and simplifying assumptions that are included essentially defines a different modeling approach, and no one can a priori be considered better or worse than any other one.

• *Rapidly changing washcoat technology*. Catalytic converter manufacturers continuously improve the chemical characteristics of the catalytic converter washcoats, in an effort to produce efficient as well as low-cost designs. Thus chemical kinetics research has to keep track of most modern washcoat developments, which inhibits the acquisition of in-depth knowledge about the washcoats chemical behavior and may lead to system-specific conclusions and results.

• *Performance assessment difficulty*. Finally, there is no consensus on how to assess model performance, so that models with similar scope can be compared. The introduction of such a methodological tool should help towards identifying the weaknesses and advantages of different approaches and provide with a quantitative criterion for model comparison.

The variety of modeling approaches that have been proposed and tested until today can be largely attributed to the above points. Nevertheless, similarities may be noticed among many different models and the majority of them share a common structure, which is dictated by the structure and operating concept of the catalytic converter itself.

Specifically, the catalytic converter is essentially a batch of parallel channels, which have been covered in their interior by a chemically active washcoat layer. The structure of most published models follows the structure of the converter itself so that each model can be divided into three distinct levels: The washcoat level, the channel level, and the reactor level. Below, we attempt to clarify what is modeled at each level and discuss which are the most common choices that one has to make when developing a catalytic converter model.

Washcoat Level. Washcoat modeling is local in nature. At this level, local phenomena at each point of the washcoat along the channel axis are considered. Two dominant phenomena should be modeled: diffusion and simultaneous reaction within the washcoat.

Heat and mass transport through the boundary layer of the flow is normally accounted for by employing mass and heat-transfer coefficients. Heat transfer through the washcoat is normally omitted, since the washcoat is approximately isothermal [24]. Finally, several approaches exist for the modeling of mass transport through the washcoat: from completely neglecting washcoat diffusion to detailed calculation of species profiles diffusing–reacting in the washcoat solving the corresponding balance equations. The former can be viewed as a zero-dimensional approach, while the latter is one- or two-dimensional and implies significant added computational cost.

For the reaction modeling, the mission of the model is twofold:

(i) To identify the prevailing physical and chemical phenomena and formulate an appropriate reaction scheme.

(ii) To assign a rate expression to each reaction.

When building the reaction scheme, the primary choice is between elementary or overall reactions. Elementary reactions describe in detail the real steps with which heterogeneous catalysis proceeds. On the other hand, overall reactions view heterogeneous catalysis phenomenologically as a one-step reaction and no intermediate steps are considered.

Elementary reactions usually employ simple Arrhenius-type rate expressions [25,26]. Overall reactions use more complicated rate expressions, which are either totally empirical or they are based on the Langmuir-Hinshelwood formalism and containing some empirical terms [9,12,27]. Essentially, the overall reaction approach favours the simplification of the reaction scheme, at the expense of using more complicated and highly empirical rate expressions; in a sense, the complexity of the reaction scheme details is hidden into the mathematical formulation of the rate expressions. An interesting fact that is not yet fully understood by fundamental researchers in chemistry and chemical kinetics is that the above-mentioned engineering approach has succeeded in producing unexpectedly high accuracy in matching the performance of catalytic converters in real cycles [7,23].

Channel Level. At the channel level, the local information provided by the washcoat model is exploited. The objectives of the model are the following:

(i) to determine the mass and heat transfer between the exhaust gas and the solid phase (substrate and washcoat) of the converter;

(ii) to determine the exhaust gas characteristics (temperature and species concentrations) along the channel.

At this level, chemical and physical phenomena in the washcoat are viewed as heat or mass sinks/sources. Profiles of gas temperature and species concentration between the channel wall and the bulk flow are computed along the channel axis.

The exhaust gas flow through the channel is laminar and is usually approximated with plug flow. Thus one-dimensional heat and mass balance equations for the exhaust gas are formulated at this level of modeling. The option here is between a transient and a quasisteady approach. If transient (time-dependent) terms of the equations are omitted, steady-state balances remain. The quasisteady approach implies that these steady-state balances are solved for each time step as solution proceeds in time for different boundary conditions. The boundary conditions are imposed by the transient reactor model.

By omitting transient terms, the steady-state approach essentially assumes that the there is no accumulation of heat or mass in the gas flow, which is a realistic assumption [28]. The objective of this approximation is to simplify the balance equations and reduce the computational cost that is involved in their solution.

Reactor Level. At the reactor level, channel-level information is exploited. Specifically, channels interact with each other only via heat transfer. Thus channels are viewed as heat sinks/sources and only one problem is tackled: Heat transfer in the solid phase, i.e., conductive heat transfer in the monolith and convection–radiation to the surrounding air. At this level, the heat sources computed for each channel at the kinetics and channel level calculations are used to estimate the temperature field of the monolith.

Heat-transfer calculations may be one, two, or three dimensional, depending on the desired accuracy. One-dimensional (1D) reactor level models treat all the channels of the monolith identically (i.e., subject to identical boundary conditions). On the other hand, 2D computations divide the monolith into sectors (clusters of channels) and the channel level computations are done for each one of the distinct sectors [10]. Finite-volume or finite element approaches may be employed in the 3D computation [6,11,15].

Evidently, each catalytic converter model incorporates a lot of assumptions and approximations. At each level of catalytic converter modeling, choices have to be made regarding modeling complexity and detail, which affect the accuracy and applicability of the resulting model. For the engineer, modeling detail is always dictated by the engineered object. Thus before deciding for a specific model formulation, the model's purpose should be clarified. Therefore we give below a brief discussion about the role of catalytic converter modeling within the process of modern exhaust aftertreatment systems design and operation.

Role of Modeling in the Design of Ultra Low Emission Exhaust Aftertreatment Systems

According to emission legislations for passenger cars and vans, emissions are measured over an engine or vehicle test cycle, which is an important part of every emission standard. These test

cycles are supposed to create repeatable emission measurement conditions and, at the same time, simulate a real driving condition of a given application.

Consequently, the primary objective of the automotive industry is to build cost-effective exhaust lines that will enable the vehicle to succeed in the legislated driving cycle tests. Because of the increasingly stringent emission standards, we observe a trend towards more complicated exhaust lines. For successful design, the engineer must consider not only the catalytic converter but, instead, the exhaust line (engine settings and control–exhaust piping–catalytic converter) as a system—an exhaust aftertreatment system. This progressively makes the experimental testing of the exhaust line more difficult and more expensive, requiring more time and experimental data to tune it appropriately.

In order to decrease cost and design time for development, modeling of the whole exhaust aftertreatment system would be extremely helpful. If fast, reliable models were available to the industry, new exhaust line configurations could be tested rapidly and at a reasonable cost; additionally, optimization of the exhaust line components could be aided by numerical optimization procedures to achieve improved configurations and lower overall emissions. The underlying notion is the incorporation of computer-aided engineering (CAE) practices in the design of exhaust lines, which is currently under way in the automotive industry.

Consequently, the targets for the exhaust line modeling are set by the industry. Currently, an indicative wish list for an ideal modeling tool of the kind is the following:

• *Reliability*. It should be cross checked and validated thoroughly in real-world case studies before conclusions and design decisions can be drawn using it.

• *Speed*. It should run reasonably fast (that is, faster than real time), with common computer equipment so that it can be tested, adjusted, and used within the time and cost constraints of the automotive industry.

• *Versatility*. It should be easy to modify and apply to different system configurations, in order to enable their assessment and tuning.

• *Ease of use*. It should be easy to validate and use by automotive engineers who are not modeling experts.

• *Minimum input data*. It should require input data that may be acquired by routine experiments, in order to keep cost low and to prevent input data uncertainty and errors.

• *Simplicity*. It should follow the fundamental engineering rule of thumb to keep complexity low. In this way, engineers–users can easily have control over their modeling tools and easily gain insight to model behavior and results.

Traditionally, modeling tools and CAE procedures in general are used in many areas of automobile design. The modeling of the catalytic converter proved to be a very complex problem, though, and this area resisted the extensive application of modeling. As of today, such modeling tools are not fully accepted in the field of catalytic converter optimization, let alone the CAE-driven design of the whole exhaust line.

Nevertheless, progress on this field of research is fast. The automotive industry clearly identifies the importance of modeling tools and recent improvements of catalytic converter models are a response to this trend. Below, we present some work in this direction. We employ an updated version of a catalytic converter modeling code, which has been continuously developed since 1996 [10] and has been employed on various design projects. The software is combined with the development of a performance measure for the assessment of modeling quality, which is utilized within a genetic algorithm optimization procedure for the computer-aided estimation of reaction kinetics parameters. Our purpose is to provide a demonstration of the role and applicability of current modeling software in the design process of modern exhaust aftertreatment systems.

Model Description

Below, we present an updated version of the CATRAN catalytic converter model. The model's design concept is the minimization of degrees of freedom and the elimination of any superfluous complexity in general. The main features of the model are the following:

• transient, one-dimensional temperature profile for the solid phase of the converter (reactor level modeling);

• quasisteady, 1D computation of temperature and concentration axial distributions for the gaseous phase (channel level modeling);

• simplified reaction scheme featuring a minimum set of redox reactions and an oxygen storage submodel (washcoat level modeling).

Below, the detailed description of model formulation is given for each modeling level.

Washcoat Level Modeling. The first task of washcoat modeling is to define how the simultaneous phenomena of diffusion and reaction in the washcoat will be taken into account. What will be adopted in this work is the ''film model'' approach, which is the simplest and most widely used one (e.g., Refs. [9], [11]). The film model approximates the washcoat with a solid–gas interface, where it is assumed that all reactions occur. This approximation essentially neglects diffusion effects completely, and assumes that all catalytically active cites are directly available to gaseous-phase species at this solid–gas interface.

This has been questioned by Zygourakis and Aris [24] and Hayes and Kolaczkowski [29]. They provide evidence that concentration gradients in the washcoat are present and may significantly affect the operation of the monolithic converter, especially in high temperatures. Nevertheless, significant complexity is introduced in the models in order to explicitly consider diffusion in the washcoat. Therefore washcoat diffusion is not implemented here and its effect is lumped into the kinetic parameters of the model.

The approximation for the solid–gas interface states that all species that diffuse to it through the boundary layer are removed from the gas phase due to reactions:

$$\frac{\rho_g}{M_g} k_{m,j} S (c_j - c_{j,s}) = R_j . \tag{1}$$

The left-hand side of the above equation describes mass transfer through the boundary layer of the gas flow. Parameter k_m is the mass transfer coefficient in the boundary layer, c_j denotes species concentration at the gaseous phase, and $c_{s,j}$ is corresponding concentration at the gas–solid interface. S is the geometrical surface area of the washcoat, i.e., channel wall area per channel volume. For a channel with hydraulic diameter d_h, we readily find: $S = 4/d_h$.

On the right-hand side of Eq. (1), the rate R_j refers to the production or consumption of each species at the solid–gas interface. For N_R reactions, each taking place with a rate r_k, the rate of consumption or production of a species j is

$$R_{\mathrm{rea},j} = \delta \gamma S \sum_{k=1}^{N_R} (a_{j,k} r_k), \tag{2}$$

where $a_{j,k}$ is the stoichiometric coefficient of species j in reaction k, δ is the washcoat thickness, and γ is the specific catalyst area, i.e., catalytically active area per washcoat volume.

The second task of washcoat modeling is to choose a reaction scheme and the appropriate expressions for the reaction rates r_k. We opt for overall reactions, because they provide the user with a more compact and comprehensible reaction scheme and they are computationally less expensive. Here, the three-way catalytic converter (3WCC) will be considered, which is designed for spark-ignition engines exhaust. Below, we briefly discuss what we choose to implement in this case.

Table 1 Reaction scheme and rate expressions of the model

	Reaction	Rate expression
	Oxidation reactions	
1	$CO+1/2O_2 \rightarrow CO_2$	$r_1=\frac{A_1 e^{-E_1/R_gT} c_{CO} c_{O_2}}{G}$
2	$H_2+1/2O_2 \rightarrow H_2O$	$r_2=\frac{A_2 e^{-E_2/R_gT} c_{H_2} c_{O_2}}{G}$
3, 4	$C_\alpha H_\beta+(\alpha+0.25\beta)O_2 \rightarrow \alpha CO_2+0.5\beta H_2O$	$r_k=\frac{A_k e^{-E_k/R_gT} c_{C_\alpha H_\beta} c_{O_2}}{G}, \quad k=3,4$
	NO reduction	
5	$2CO+2NO \rightarrow 2CO_2+N_2$	$r_5=A_5 e^{-E_5/R_gT} c_{CO} c_{NO}$
	Oxygen storage	
6	$2CeO_2+CO \rightarrow Ce_2O_3+CO_2$	$r_6=A_6 e^{-E_6/R_gT} c_{CO} \psi \Psi_{cap}$
7, 8	$C_\alpha H_\beta+(2\alpha+\beta)CeO_2 \rightarrow$ $\rightarrow(\alpha+0.5\beta)Ce_2O_3+\alpha CO+0.5\beta H_2O$	$r_k=A_k e^{-E_k/R_gT} c_{C_\alpha H_\beta} \psi \Psi_{cap}, \; k=7, 8$
9	$Ce_2O_3+1/2O_2 \rightarrow 2CeO_2$	$r_9=A_9 e^{-E_9/R_gT} c_{O_2} (1-\psi) \Psi_{cap}$
10	$Ce_2O_3+NO \rightarrow 2CeO_2+1/2N_2$	$r_{10}=A_{10} e^{-E_{10}/R_gT} c_{NO} (1-\psi) \Psi_{cap}$
	Inhibition term	
	$G=T(1+K_1 c_{CO}+K_2 c_{CxHy})^2 (1+K_3 c_{CO}^2 c_{CxHy}^2)(1+K_4 c_{NO}^{0.7}), \quad K_i=k_i \exp(-E_i/R_gT)$	
	$K_1=65.5 \quad K_2=2080 \quad K_3=3.98 \quad K_4=4.79\times 10^5$	
	$E_1=-7990 \quad E_2=-3000 \quad E_3=-96{,}534 \quad E_4=31{,}036$	
	Auxiliary quantities	
	$\psi=\frac{2\times \text{moles } CeO_2}{2\times \text{moles } CeO_2+\text{moles } Ce_2O_3}, \quad \frac{d\psi}{dt}=-\frac{r_9+r_{10}}{\Psi_{cap}}+\frac{r_6+r_7+r_8}{\Psi_{cap}}$	

In the present model, the oxidation reactions rates of CO and HC are based on the expressions by Voltz et al. [27]. It is interesting to note that the expressions developed by Voltz et al. about 30 years ago for a Pt oxidation catalyst continue to be successful, with little variation, in describing the performance of Pt:Rh, Pd, Pd:Rh, and even tri-metal catalysts. For the HC oxidation, we have to note the real exhaust gas contains a very complex mixture of several hundreds of different hydrocarbon species with variability in composition depending on the driving conditions [30]. In practice, the diversity of the HC mixture is usually taken into account by considering two categories of hydrocarbons, each being oxidized in different temperature: an easily oxidizing HC (''fast'' HC), and a less-easily oxidizing HC (''slow'' HC). Here, the ''fast'' HC is represented by propene (C_3H_6) and the ''slow'' HC is represented by propane (C_3H_8). In practice, only the total hydrocarbon content of the exhaust is measured. Throughout this work, it is assumed that the exhaust HC consisted of 85% ''fast'' HC and 15% ''slow'' HC. This assumption was done for modeling purposes due to the lack of more accurate data and, according to our experience, it gives satisfactory results.

For the reaction between CO and NO we use an empirical reaction rate adopted from Pattas et al. [31], which predicts a variable order of reaction for the CO oxidation from NO, depending on CO concentration. The expression is qualitatively consistent with the results of Koberstein and Wannemacher [32], which predict that the reaction order for CO in the CO–NO reaction tends to unity as the reactants' concentrations tend to vanish. Finally, hydrogen oxidation is also included in the model.

All reduction–oxidation reactions employed in the model, along with their rate expressions, are given in Table 1.

Apart from the redox reactions, oxygen storage phenomena play a principal role in the efficiency of the 3WCC. Oxygen storage occurs on the ceria (Ce), which is contained in large quantities in the catalyst's washcoat (at the order of 30% wt). Under net oxidizing conditions, 3-valent Ce oxide (Ce_2O_3) may react with O_2, NO, or H_2O and oxidize to its four-valent state (CeO_2). Under net reducing conditions, CeO_2 may function as an oxidizing agent for CO, HC, and H_2.

Oxygen storage is taken into account by an updated reaction scheme. The new scheme consists of five reactions which account for (i) Ce_2O_3 oxidation by O_2 and NO, and (ii) CeO_2 reduction by CO and fast/slow hydrocarbons The model uses the auxiliary quantity ψ to express the fractional extent of oxidation of the oxygen storage component. It is defined as

$$\psi=\frac{2\times \text{moles } CeO_2}{2\times \text{moles } CeO_2+\text{moles } Ce_2O_3}. \tag{3}$$

The extent of oxidation ψ is continuously changing during transient converter operation. Its value is affected by the relative reaction rates of reaction nos. 6–10. The rates of reactions, also given in Table 1, are expected to be linear functions of ψ. Specifically, the oxidation rate of the oxygen storage component is assumed proportional to the active sites of Ce_2O_3, i.e., to $\Psi_{cap}(1-\psi)$. On the other hand, the oxidation rate of CO and HC by CeO_2 is assumed proportional to ($\Psi_{cap}\psi$). Moreover, the rates of these reactions should be linearly dependent on the local concentration of the corresponding gaseous phase reactant.

The rate of variation of ψ is the difference between the rate that Ce_2O_3 is oxidized and reduced:

$$\frac{d\psi}{dt}=-\frac{r_9+r_{10}}{\Psi_{cap}}+\frac{r_6+r_7+r_8}{\Psi_{cap}}. \tag{4}$$

The updated model includes an analytical solution for Eq. (4) for ψ at each node along the catalyst channels.

Channel Level Modeling. For the formulation of the channel-level model, two usual simplifications are employed [26,33], namely:

• The axial diffusion of mass and heat in the gas phase is negligible.

• The mass and heat accumulation in the gas phase is negligible. (This comprises the assumption for the quasi-steady-state nature of the problem.)

The first assumption is generally accepted and is employed in most models, e.g., those of Chen et al. [11] and Siemund et al. [9]. Only the boundary layer effect on mass transfer is accounted for, using a mass transfer coefficient k_m, which is a function of the Sherwood number. Bulk flow is approximated with plug flow with uniform temperature T_g and species concentrations c_j. The velocity of the flow readily results from the mass flow rate: $u_z = 4\dot{m}/(\rho \pi d_h^2)$.

The second assumption is more controversial and both the quasi-steady and the transient approach have been tested in the literature. Shamim et al. [15] have presented a model that incorporates transient terms at channel level modeling. On the other hand, Young and Finlayson [8] and Oh and Cavendish [3] argue about the validity of the quasi-steady approximation. They provide justification on the basis of the large ratio of thermal to mass time constants of the problem. Following this line of thought, the quasi-steady approach is used here as well, for simplicity and low computational cost.

In order to write the mass balance for the exhaust gas, a mean bulk value c_j is employed for the gas–phase concentration of each species. Likewise, a value $c_{s,j}$ is considered for the concentration of each species at the solid–gas interface. Using the quasi-steady-state approximation and neglecting diffusion and accumulation terms, the mass balance for the gas phase becomes

$$\rho_g u_z \frac{\partial c_j(z)}{\partial z} = \rho_g k_{m,j} S[c_j(z) - c_{s,j}(z)]. \tag{5}$$

Similarly to the above, a mean bulk value T_g is used for the exhaust gas temperature, and a solid phase temperature T_s is introduced for the monolith and the solid–gas interface. Energy is transferred to and from the exhaust gas only due to convection with the channel walls. Thus the energy balance for the gas phase becomes

$$\rho_s c_p u_z \frac{\partial T_g(z)}{\partial z} = hS[T_s(z) - T_g(z)]. \tag{6}$$

Parameter h is the heat-transfer coefficient and is calculated as a function of the Nusselt dimensionless number.

Finally, the boundary conditions for the temperature, mass flow rate, and concentrations are given from measurement at the converter's inlet:

$$\begin{aligned} c_j(t, z=0) &= c_{j,\text{in}}(t), \\ T_g(t, z=0) &= T_{g,\text{in}}(t), \\ \dot{m}(t, z=0) &= \dot{m}_{\text{in}}(t). \end{aligned} \tag{7}$$

The species that are considered in the exhaust gas flow are the following: $j = \text{CO}, \text{O}_2, \text{H}_2, \text{HC}_{\text{fast}}, \text{HC}_{\text{slow}}, \text{NO}_x, \text{N}_2$.

Reactor Level Modeling. At the reactor level modeling, heat transfer between channels and between the reactor and its surrounding are modeled. The principal issue here is to decide if one-, two-, or three-dimensional modeling of the heat transfer should be employed.

The reactor model presented in this work is a one-dimensional heat-transfer model for the transient heat conduction in the monolith. Heat losses to the environment via convection and radiation are also taken into account. Its primary assumptions are the following:

• Heat losses from the front and the rear face of the monolith are neglected. (To our knowledge, this is the case with all models that have appeared in the literature.)

• Since the catalytic converter is always insulated, simpler models approximate the convert as adiabatic. Heat losses to the surrounding are taken into account but, owing to the model's 1D nature, they are inevitably distributed uniformly in each monolith's cross section.

• Flow rate and temperature profiles of the exhaust gas at the inlet of the filter are considered uniform. An average value for flow rate and temperature is measured, and gas flow is distributed uniformly to each channel.

The temperature field in the converter is described by the equation of transient heat conduction in one dimension, with heat sources being convection from the exhaust gas, the enthalpy released from the reactions, and convection to ambient air,

$$\rho_s c_{p,s} \frac{\partial T_s}{\partial t} = k_{s,z} \frac{\partial^2 T_s}{\partial z^2} + hS(T_g - T_s) + \sum_{k=1}^{N_R} (-\Delta H_k) r_k + Q_{\text{amb}}. \tag{8}$$

Finally, the boundary condition needed for the solution of the heat conduction equation refers to the heat losses to ambient air:

$$Q_{\text{amb}} = S_{\text{mon}}[h_{\text{amb}}(T_s - T_{\text{amb}}) + \varepsilon \sigma (T_s^4 - T_{\text{amb}}^4)]. \tag{9}$$

Two- and three-dimensional reactor models have also appeared in the literature, e.g., the models of Heck et al. [34], Chen et al. [11], Zygourakis [35], and Jahn et al. [36]. These models are indispensable if the exhaust gas at the converter inlet exhibits a severely nonuniform flow profile but also require mass flow rate and temperature profiles at the inlet of the catalytic converter. Such data are not usually available in routine engine-bench or driving cycle converter tests, which are the main application field for our model. Therefore the 1D approach is preferred, since its modeling detail matches routine input data quality, provides sufficient accuracy, and has low computational power requirements.

Tuning Procedure

General. The kinetics submodel introduces into the catalytic converter model a set of parameters that have to be estimated with reference to a set of experimental data. The introduction of tunable parameters is inevitable regardless of the formulation of the reaction scheme. Tunable parameters take into account the reactivity of the specific washcoat formulation as well as any other aspect of catalytic converter operation that is not included in the model explicitly.

In the present model, the tunable parameters are the activation energy E_k and the preexponential factor A_k that are included in the reaction rate r_k of each reaction k. In total, there is a maximum number of 20 tunable parameters, however, the values of activation energies are more or less known from Arrhenius plots and thus only the pre-exponential factors are tuned (ten tunable parameters). Apart from reaction activity, tunable parameters values include the approximations that have been done during model formulation. Among them, the most important are:

• effect of reaction scheme and rate expressions simplifications;
• effect of exhaust gas input data uncertainty;
• effect of neglection of diffusion in the washcoat;
• effect of 1D reactor model approximation.

Since (i) the rate expressions of the model are empirical and (ii) effects of model approximations are lumped into the tunable parameters, the latter do not correspond to real kinetic parameters. Rather, they should be viewed as fitting parameters of the model.

The traditional method to tune a model was to manually adjust the parameters by a trial-and-error procedure, starting from a set of realistic values (known from previous experience) and modifying them gradually, so that the model results compare well with the measured ones. The usual method for computation versus measurement comparison is inspection of plotted results. Thus manual tuning introduces human intuition and experience in order to (i) assess model performance, and (ii) fit the model to the given experimental data. This is a questionable practice because

• inspection is dependent on the scale that results are viewed and it may therefore be misleading;

• there is considerable difficulty to compare the performance of different models that are presented in the literature;

• it does not provide any confidence about the quality of the tuning.

The above drawbacks of manual performance assessment and parameter tuning have led to efforts for the development of a corresponding computer-aided procedure. Since model tuning is essentially a parameter-fitting problem, the underlying idea of all attempts has been to express the problem mathematically as an optimization problem. This involves the introduction of an iterative optimization method, which maximizes or minimizes an objective function that indicates goodness of fit. The objective function required by the optimization procedure is thus a *performance measure* of the model, i.e., a mathematical measure that assesses a model's performance in a quantitative manner.

A few attempts for the development of a complete computer-aided tuning methodology have been presented in the past. Montreuil et al. [12] were the first to present a systematic attempt for the tuning of the parameters of their steady-state three-way catalytic converter model. Dubien and Schweich [37] also published a methodology to determine the pre-exponential factor and the activation energy of simple rate expressions from light-off experiments. Pontikakis and Stamatelos [7,38] introduced a computer-aided tuning procedure for the determination of kinetic parameters of a three-way catalytic converter model from driving cycle tests based on the conjugate gradients method. Glielmo and Santini [39] presented a simplified three-way catalytic converter model oriented to the design and test of warm-up control strategies and tuned it using a genetic algorithm.

All of the above efforts used a performance measure based on the least-squares error [40] between measured and computed results. Except for Glielmo and Santini, all other works are based on gradient-based methods for the optimization of the performance measure [41]. Gradient methods are faster, more accurate, and may be used as black-box methods, but assume that the optimization space is unimodal (i.e., it contains a single extremum). Genetic algorithms, used by Glielmo and Santini, are better suited to multi-modal optimization but they are slower, less accurate, and have to be appropriately adapted to the target problem.

In the present work, we present recent progress that has been made in the field of computer-aided parameter estimation. It is a continuation of the work of Pontikakis and Stamatelos [7] and updates both performance measure definition and optimization methodology. In the following sections the requirements that a performance measure should comply with are presented, and a performance measure that satisfies these requirements is defined. Finally, a genetic algorithm is applied as an optimization methodology [23].

Formulation of the Performance Measure. The performance measure that is formulated below exploits the information of species concentrations measurements at the inlet and the outlet of the catalytic converter. Specifically, it is based on the conversion efficiency E_j for a pollutant j. Herein, we take into account the three legislated pollutants, thus $j=\mathrm{CO},\ \mathrm{HC},\ \mathrm{NO}_x$.

To account for the goodness of computation results compared with a measurement that spans over a certain time period, an error e for each time instance must be defined. The latter should give the deviation between computation and measurement for the conversion efficiency E. Summation over time should then be performed to calculate an overall error value for the whole extent of the measurement. Here, the error is defined as

$$|e| = |E - \hat{E}|. \tag{10}$$

Absolute values are taken to ensure error positiveness. This error definition also ensures that $0 \leqslant |e| \leqslant 1$, since it is based on conversion efficiency.

The error between computation and measurement is a function of time and the tunable paremeter vector: $e=e(t;\vartheta)$, where ϑ is the formed by the pre-exponential factor and activation energy of each reaction of the model:

$$\vartheta = [A_1, E_1, A_2, E_2, \ldots, A_{N_P}, E_{N_P}]^T. \tag{11}$$

We name *performance function* $f(t;\vartheta)=f(e(t;\vartheta))$ a function of the error e, which is subsequently summed over some time period τ to give the performance measure F. Here, the performance function is defined as

$$f(t_n;\vartheta) = \frac{|e(t_n;\vartheta)|}{e_{\max}(t_n)}. \tag{12}$$

Time t take discrete values, $t_n = n\Delta t$, with Δt being the discretization interval which corresponds to the frequency data measured. The quantity $e_{\max}$ is the maximum error between computation and measurement, and it is defined as

$$e_{\max}(t_n) = \max\{\hat{E}(t_n), 1-\hat{E}(t_n)\}. \tag{13}$$

The performance measure can be subsequently formed using some function of the sum of the performance function over time:

$$F(\vartheta) = F\left(\sum_{n=0}^{N} f(t_n;\vartheta)\right), \quad N = \tau/\Delta t. \tag{14}$$

In this work, we define the performance measure F as the mean value of the performance function over the time period of interest:

$$F(\vartheta) = \frac{1}{N}\sum_{n=0}^{N} f(t_n;\vartheta) = \frac{1}{N}\sum_{n=0}^{N} \frac{|e(t_n;\vartheta)|}{e_{\max}(t_n)}. \tag{15}$$

The performance measure defined in Eq. (15) is used for the assessment of the performance of each of the three pollutants CO, HC, NO_x. The total performance measure is computed as the mean of these three values:

$$F = \frac{F_{\mathrm{CO}} + F_{\mathrm{HC}} + F_{\mathrm{NO}_x}}{3}. \tag{16}$$

The above performance measure presents advantageous features compared to the classical least-squares performance measure:

• It ranges between two, previously known, finite extreme values. Extremes correspond to zero and maximum deviation between calculation and experiment.

• The extrema of the performance measure are the same for all physical quantities that may be used and all different measurements where the performance measure may be applied. That is, the performance measure is normalized so that its extrema do not depend on the either the measured quantities or the experimental protocol.

Furthermore, out of the different versions of performance measure tested within the specific genetic algorithm optimization procedure, the specific one gave us the best convergence, without the need to rely on empirical weight factors [23].

Optimization Procedure. Having defined the performance measure for the model, the problem of tunable parameter estimation reduces in finding a tunable parameter vector ϑ that maximizes F.

The parameter vector ϑ is not used directly in the optimization procedure. Instead, we perform parameter reparametrization for the pre-exponential factor A, defined as

$$A = 10^{\tilde{A}} \Leftrightarrow \tilde{A} = \log A \tag{17}$$

and the transformed tunable parameters vector becomes

$$\tilde{\vartheta} = [\tilde{A}_1, E_1, \tilde{A}_2, E_2, \ldots, \tilde{A}_{N_P}, E_{N_P}]^T. \tag{18}$$

Then, the problem of tunable parameter estimation is expressed as

Table 2 Parameters of the genetic algorithm

Encoding type	binary
Crossover operator	one-point crossover
Mutation operator	binary mutation
Population size	100
Crossover probability	0.6
Mutation probability	0.03
Encoding resolution	10 bit ($\ell=10$)
Limits	$10^{07}<A_i<10^{23}$

$$\text{Maximize } F'(\tilde{\vartheta}) = 1 - F(\tilde{\vartheta}) = \frac{1}{3N} \sum_{j=\text{CO,HC,NO}_x} \sum_{n=0}^{N} \frac{|e_j(t_n;\tilde{\vartheta})|}{e_{j,\max}(t_n)}, \quad N = \tau/\Delta t. \tag{19}$$

This is a constraint maximization problem, since the components of vector ϑ are allowed to vary between two extreme values, i.e., $\vartheta_{i,\min} \leqslant \vartheta_i \leqslant \vartheta_{i,\max}$. Previous experience [7] has shown that the parameter space that results from this problem formulation is multimodal. Thus an appropriate optimization procedure should be used. Here, a genetic algorithm has been employed for the maximization of Eq. (19). A brief description of the genetic algorithms operation concept and the main features of the implementation used herein are presented below.

A genetic algorithm is a kind of artificial evolution. What evolves is a population of solutions to a problem; each solution is an individual of the population. Individuals are born, mate, reproduce, are mutated, and die analogously to nature's paradigm. The cornerstone of this evolution process is that more fit individuals are given more advantage to live longer and propagate their genetic material to the next generations.

The main steps taken by the algorithm are the following:

(i) *Initialization*. A set of points in the optimization space is chosen at random. This is the initial population of the genetic algorithm, with each point corresponding to an individual of the population.

(ii) *Encoding*. Each individual is encoded to a finite binary string (chromosome). In brief, each real interval $\lfloor \tilde{\vartheta}_{i,\min}, \tilde{\vartheta}_{i,\max} \rfloor$ is mapped to the integer interval $[0,2^{\ell}]$ and subsequently transform from integer to binary. Then, the chromosome is built by concatenating the binary strings that correspond to the value of each parameter ϑ_i. This encoding is called "concatenated, multiparameter, mapped, fixed-point coding" [42].

(iii) *Fitness calculation*. The fitness of each individual in the population is computed using Eq. (19). It should be noticed that fitness calculation requires that the model be called for each individual, i.e., as many times as the population size.

(iv) *Selection*. Random pairs of individuals are subject to tournament, that is, mutual comparison of their fitnesses [43]. Tournament winners are promoted for recombination.

(v) *Recombination (mating)*. The one-point crossover operator [42] is applied to the couples of individuals that are selected for recombination (parents). One-point crossover works on the chromosomes (binary encodings) of the individuals. The resulting chromosomes (children) are inserted to the population replacing their parents and they are decoded to produce their corresponding real parameter vector.

(vi) *Mutation*. A small part of the population is randomly mutated, i.e., random bits of the chromosomes change value.

(vii) Steps (iii)–(vii) are repeated for a fixed number of generations or until acceptably fit individual has been produced.

The randomized nature of the genetic algorithm enables it to avoid local extrema of the parameter space and converge towards the optimum or a near-optimum solution. It should be noted, though, that this feature does not guarantee convergence to the global optimum. This behavior is common to all multimodal optimization techniques and not a specific genetic algorithm characteristic.

The implementation of the genetic algorithm that was described above is not the only one possible. There are a number of design decisions and parameters that influence the operation, efficiency, and speed of the genetic algorithm. The present implementation is classical, though. Its characteristics are summarized in Table 2.

Application Examples

The model's predictive ability is going to be demonstrated in a number of typical applications. The first step is to tune the model for a specific catalyst configuration in typical driving cycle test and the estimate the kinetic parameters of the model. Successful tuning in this phase implies that (i) the model incorporates the appropriate degrees of freedom in order to match the measurement, (ii) the tuning methodology is able to tackle the parameter estimation optimization problem successfully, and (iii) experimental data are in a certain level of accuracy and has been processed through a quality assurance procedure [44].

First, a MVEG test is considered, (European test cycle). A three-way catalytic with a 2.4-l volume, two beds, 400 cpsi, 6.5-mil wall thickness, underfloor converter with 50 g/ft^3 Pt:Rh 7:1 precious metal loading is installed on a passenger car with 2-l engine displacement. The measured catalyst's performance on this car is presented in Fig. 1, by means of the measured instantaneous CO, HC, and NO_x emissions at converter inlet and exit, over the 1180-sec duration of the cycle.

Obviously, the specific converter attains a significant overall efficiency: The emissions at catalyst's exit are diminished after the cold start phase. However, the emissions standards themselves are quite low: Thus the model should not only accurately predict catalyst light-off, but it should also be capable of matching the catalyst's breakthrough during accelerations, decelerations and especially in the extra-urban, high-speed part of the cycle.

In order to match this catalyst's behavior, the model was tuned using the genetic algorithm. The measured emissions during the full NEDC were employed as a reference period for parameter estimation ($\tau=1180$ s in Eq. (19)). CPU time of the order of 48 h was required for the computation of 135 generations (100 individuals each) on a Pentium IV 2.4-GHz PC. However, if one needs faster execution time, a part of the cycle containing the cold start and some hot operation could equally do with just one-third of the time.

The tuning process resulted to the kinetics parameters of Table 3. The evolution of the most important kinetics parameters values of the individuals as determined by the genetic algorithm during the 135 generations is presented in Fig. 2. It may be observed that the genetic algorithm converges to specific values for these parameters. This behavior is not observed for all kinetics parameters, and this is taken into account for improvements in the kinetics scheme [22]. The computed results which are produced when the model is fed with the frequency factors determined by the 135th generation of the genetic algorithm, are summarized in the form of cumulative CO, HC, and NO_x emissions at catalyst's exit, compared to the corresponding measured curves in Fig. 3. The error in the prediction of cumulative emissions does not generally exceed 5% during the cycle for any species.

Also, it is useful to mention that although the specific genetic algorithm matures after about 120 generations, the convergence is clear even from the 20th generation: This means that we could compute good kinetics parameters even with 8 h CPU time. Thus the genetic algorithm approach can no more be considered as forbidding due to excessive computation time. For comparison purposes, it should be mentioned that the tuning process is the most critical part of the modeling job, and it could take several working days from experienced engineers. Moreover, its result was not guaranteed. With the new developments, whenever the genetic algorithm fails to converge, is an indication that the qual-

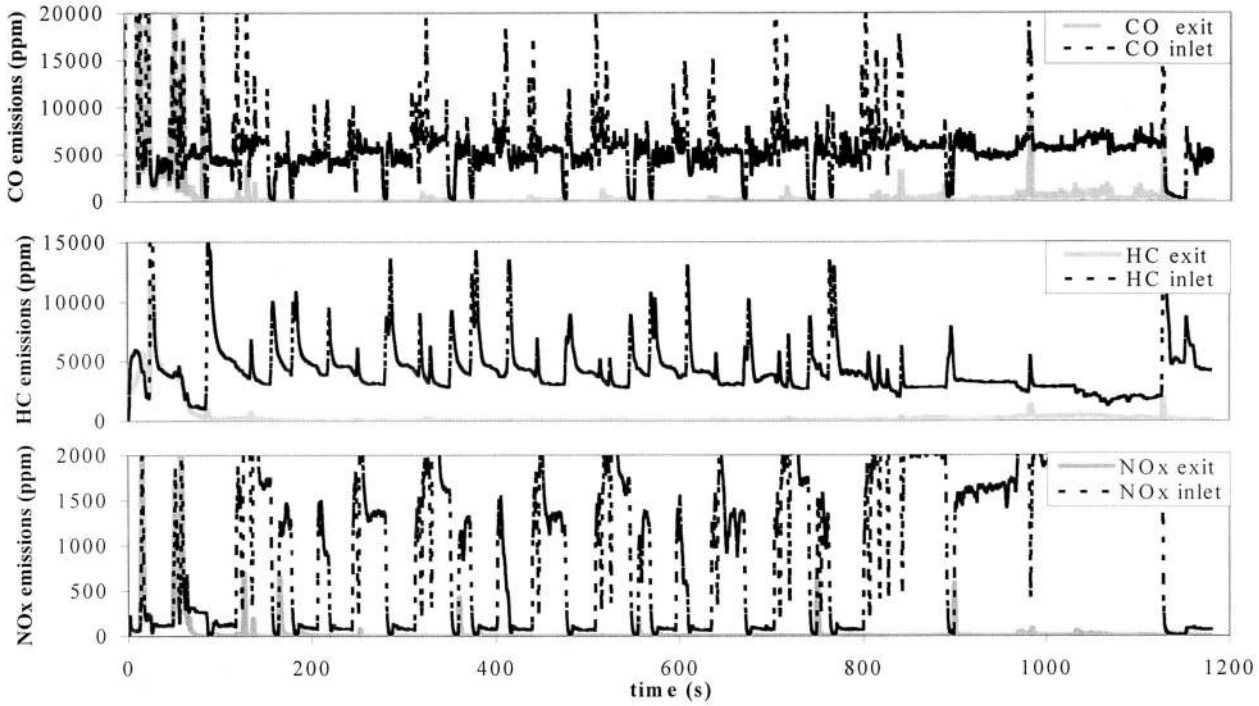

Fig. 1 Measured instantaneous CO, HC, and NO_x emissions at converter inlet and exit, over the 1180-sec duration of the cycle: 2-l-engined passenger car equipped with a 2.4-l underfloor converter with 50-g/ft^3 Pt:Rh catalyst

ity of the test data employed in the tuning process is questionable. Thus the tuning effort with the specific data is stopped and the quality assurance team must examine and possibly reject the test data [44].

In addition, computed and measured temperatures at the converter's exit are compared in Fig. 4. Apparently, the model is capable of matching the catalyst's behavior with a remarkable accuracy, allowing the performance of design optimization studies.

Since one of the objectives of this paper is to quantify the attainable accuracy, we proceed to a more detailed comparison of model predictions and measurements in the form of instantaneous CO, HC, and NO_x emissions. Prediction of instantaneous emissions over the full extent of a real legislative cycle is a significant challenge to any catalytic converter model.

Figure 5 presents the computed and measured instantaneous CO emissions at converter inlet and exit during the first 600 sec of NEDC: Apparently, the model successfully matches light-off behavior of the catalyst, as well as subsequent breakthrough during acceleration. The role of oxygen storage and release reactions in matching the CO breakthough behavior is better assessed by including in the graph the computed degree of filling of the total washcoat's oxygen storage capacity. (See, for example, the small breakthroughs, which are of the order of 200 ppm, with maximum peaks of the order of 1000 ppm, that are accurately matched by the computation).

Table 3 Kinetics parameters tuned to the Pt:Rh catalyst

	Reaction	A	E
1	$CO+1/2O_2 \rightarrow CO_2$	$2.000E+20$	90,000
2	$H_2+1/2O_2 \rightarrow H_2O$	$2.000E+19$	90,000
3, 4	$C_\alpha H_\beta+(\alpha+0.25\beta)O_2 \rightarrow \alpha CO_2+0.5\beta H_2O$	$1.800E+20$	95,000
		$2.710E+19$	120,000
	NO reduction		
5	$2CO+2NO \rightarrow 2CO_2+N_2$	$3.403E+09$	90,000
	Oxygen storage		
6	$2CeO_2+CO \rightarrow Ce_2O_3+CO_2$	$7.832E+09$	85,000
7, 8	$C_\alpha H_\beta+(2\alpha+\beta)CeO_2 \rightarrow$	$1.283E+10$	85,000
	$\rightarrow(\alpha+0.5\beta)Ce_2O_3+\alpha CO+0.5\beta H_2O$	$3.631E+13$	85,000
9	$Ce_2O_3+1/2O_2 \rightarrow 2CeO_2$	$2.553E+09$	90,000
10	$Ce_2O_3+NO \rightarrow 2CeO_2+1/2N_2$	$4.118E+10$	90,000

A comparison of computed and measured CO emissions for the cycle part from 600 to 1180 s is given in Fig. 6. In the extra-urban part of the cycle, the efficiency of the converter is reduced due to high flowrates. Again, the breakthroughs are observed when the oxygen stored in the washcoat is gradually depleted. The prediction of the model is remarkably good, especially when the order of magnitude of the breakthroughs is considered. This successful prediction indicates that the oxygen storage reactions that are implemented in the model are capable of modeling the phenomenon with high accuracy. An exception to this good behavior is observed only in the interval between 930 and 980 sec. Here there exists room for further improvement of the storage submodel and reaction scheme.

Figures 7 and 8 present the computed and measured instantaneous NO_x emissions at converter inlet and exit during the two halves of the NEDC: Apparently, the model successfully matches light-off behavior of the catalyst, as well as subsequent NO_x breakthrough behavior during accelerations. Oxygen storage is critical also here. The prediction accuracy is remarkable when one notes that the breakthroughs are of the order of a few ppm. A weak point of the model is spotted in the comparison of computed and measured behavior between 980 and 1100 sec. Again, this is the subject for future improvements in the oxygen storage submodel.

The situation appears equally good in Figs. 9 and 10 where the computed and measured instantaneous HC emissions at converter inlet and exit during the first 600 s and the rest of NEDC are given. The connection between HC breakthroughs and oxygen storage phenomena in the washcoat is apparent also in this case. The model results are of comparable quality as the previous figures, since the model predicts the events (HC breakthroughs) of the extra-urban part of the cycle, not only qualitatively, but also quantitatively, in a certain extent. HC light-off behavior is also

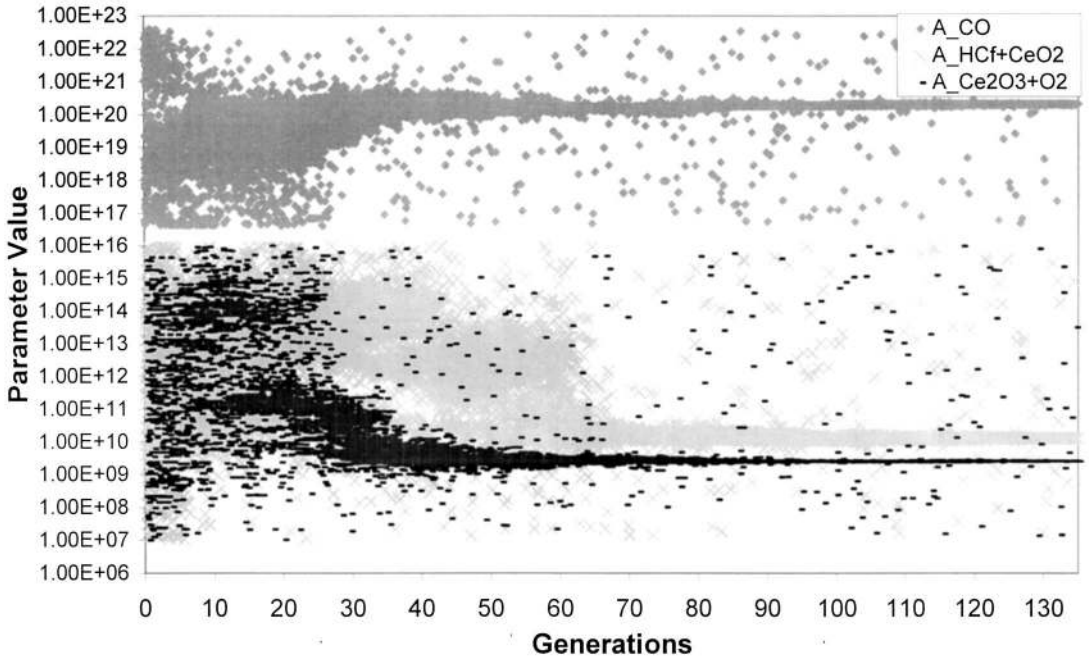

Fig. 2 Evolution of the values of three selected kinetics parameters in the 100 individuals of the population during 135 generations. The convergence to the final values is apparent even from the 40th generation.

matched with a very good accuracy, taking into account the complexity of the hydrocarbons composition that is modeled only by two representative components.

The overall performance of the specific model prediction's can be quantitatively assessed by means of evaluating the performance measure which is defined in Eqs. (15) and (16). The performance measure takes the value: $F' = 0.959$.

The above results indicate that the model formulation has the capability to match typical measurements of a three-way catalytic converter, and that the tuning methodology may be used successfully to fit the model to the measured data. Another important finding is that the model is capable of predicting the catalyst's performance outside the region where it has been tuned. That is, if we tested carrying out the tuning process based only on the first

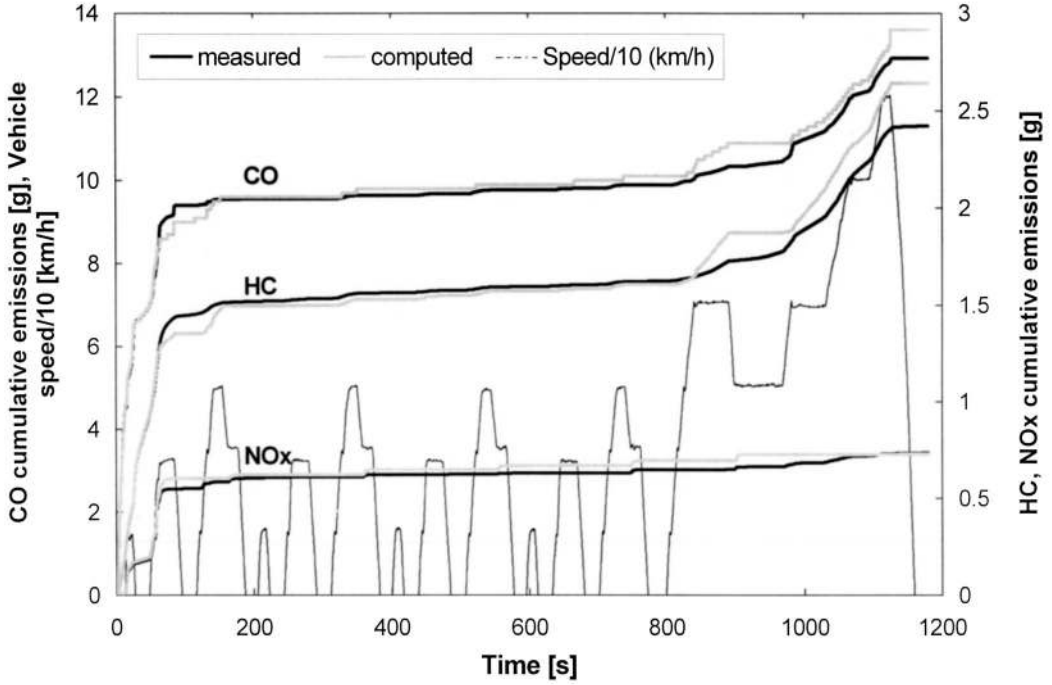

Fig. 3 Computed and measured cumulative CO, HC, and NO_x emissions at converter exit during NEDC: 2-l-engined passenger car equipped with a 2.4-l underfloor converter with 50-g/ft^3 Pt:Rh catalyst

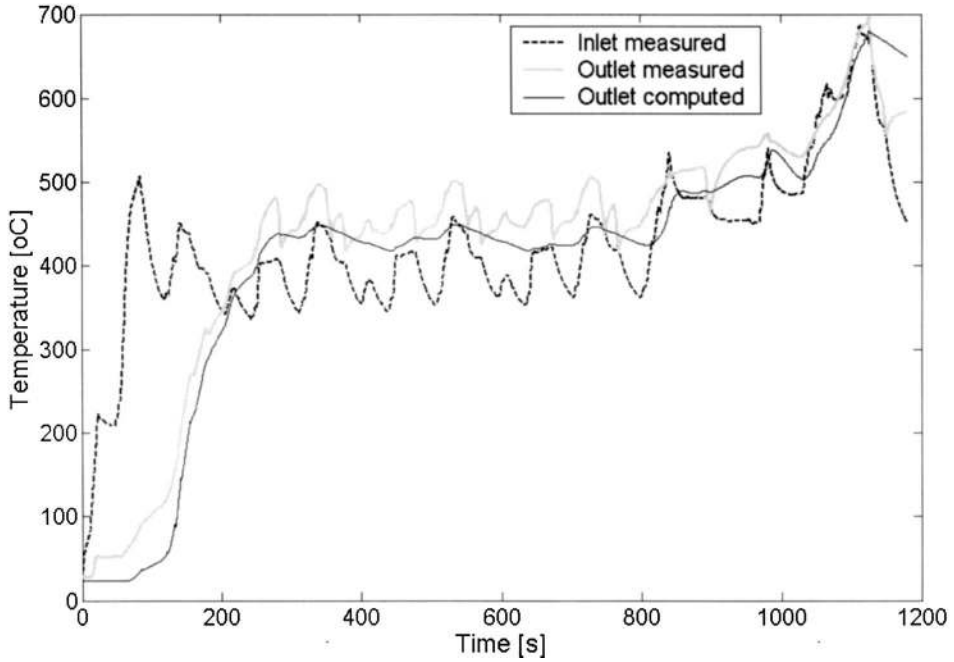

Fig. 4 Measured converter inlet temperatures, computed, and measured converter exit temperatures during NEDC: 2-l-engined passenger car equipped with a 2.4-l underfloor converter with 50-g/ft^3 Pt:Rh catalyst

400 s (see above discussion on genetic algorithm tuning), and the model demonstrated an equally satisfactory predictive ability for the catalyst performance throughout the full NEDC cycle.

Additional evidence is provided below about the model's ability to predict the operating behavior of a different catalytic converter configuration. This is achieved by using the model to predict the behavior of an alternative configuration of a three-way catalytic converter with no further kinetic parameter adjustments.

Therefore, as a next step in the assessment of the model's accuracy and predictive ability, the model is employed in the prediction of the performance of an alternative underfloor converter of the same washcoat type, which is $\frac{1}{4}$ the size of the original one.

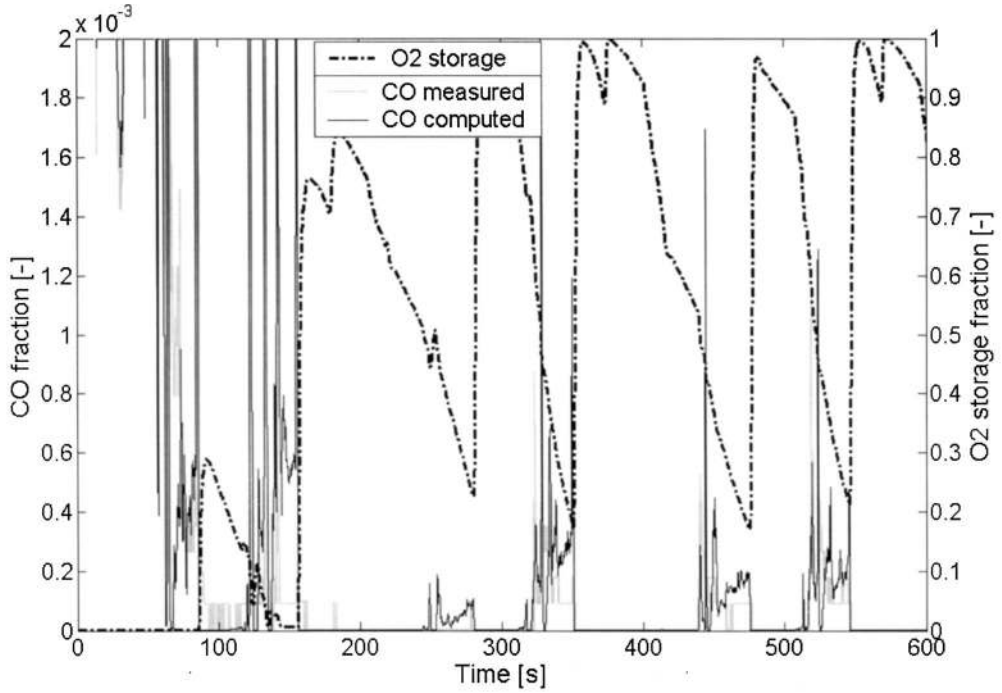

Fig. 5 Computed and measured instantaneous CO emissions at converter inlet and exit during the first 600 sec of NEDC: 2-l-engined passenger car equipped with a 2.4-l underfloor converter with 50-g/ft^3 Pt:Rh catalyst

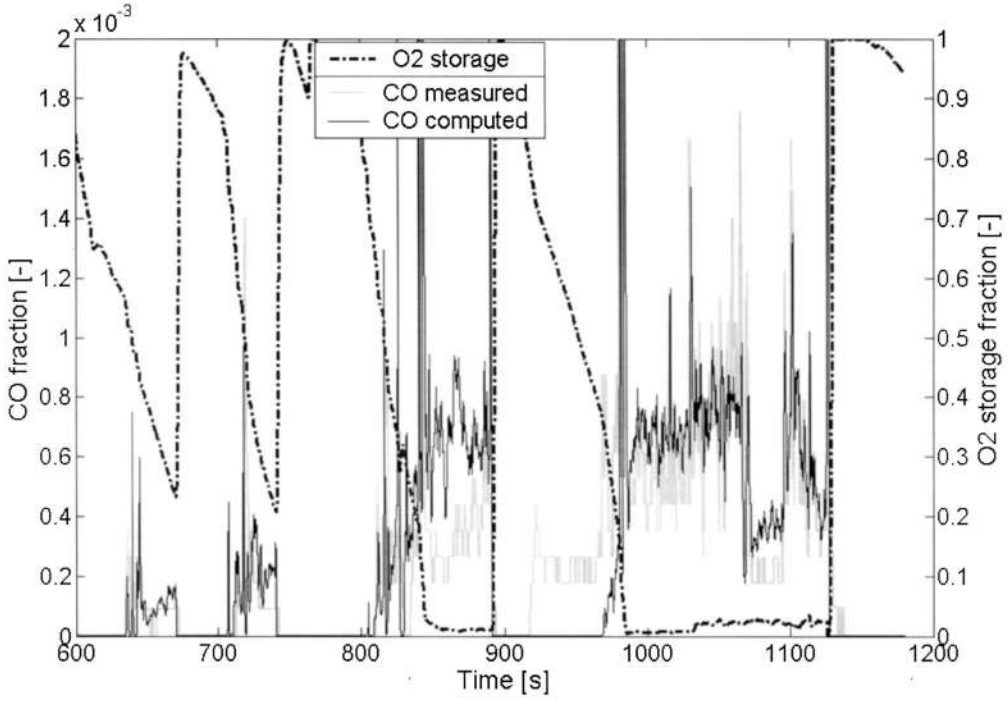

Fig. 6 Computed and measured instantaneous CO emissions at converter inlet and exit during the second half of the NEDC (600–1180 sec of NEDC): 2-l-engined passenger car equipped with a 2.4-l underfloor converter with 50-g/ft^3 Pt:Rh catalyst

Since the same catalyst formulation and precious metal loading is employed, modeling of this case is performed using the same kinetics parameters of Table 3 which where estimated for the original converter. Only the external dimensions of the converter are changed to the ones of the reduced size converter and no further tuning of the kinetic parameters is performed. The results of the model are then compared to the measured results for this converter in Fig. 11, in the form of cumulative CO, HC, and NO_x emissions. Apparently, the model is capable of predicting the significant change in all three pollutants emissions that is caused by

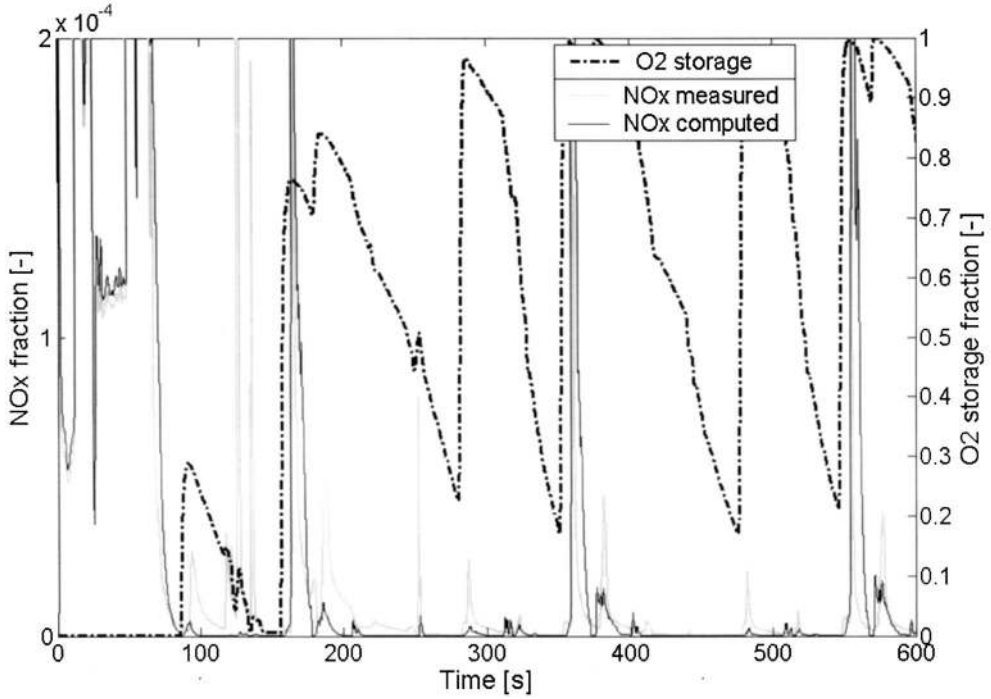

Fig. 7 Computed and measured instantaneous NO_x emissions at converter inlet and exit during the first 600 sec of NEDC: 2-l-engined passenger car equipped with a 2.4-l underfloor converter with 50-g/ft^3 Pt:Rh catalyst

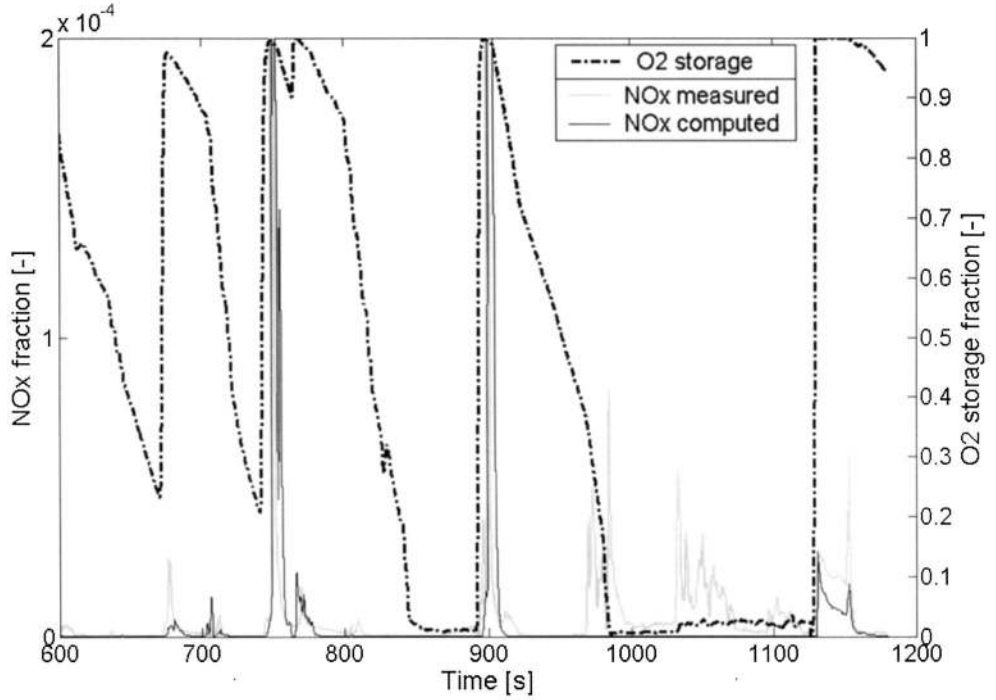

Fig. 8 Computed and measured instantaneous NO_x emissions at converter inlet and exit during the second half of NEDC: 2-l-engined passenger car equipped with a 2.4-l underfloor converter with 50-g/ft^3 Pt:Rh catalyst

the reduction of the converter's volume, without changes in its kinetic parameters. The performance measure now takes the value: $F' = 0.921$, which indicates a sufficiently accurate prediction of measured performance.

A better insight on the model's performance, also in association with oxygen storage and release behavior, can be made, for example, by a comparison of computed and measured instantaneous HC emissions at the converter's exit, during the full cycle (Fig.

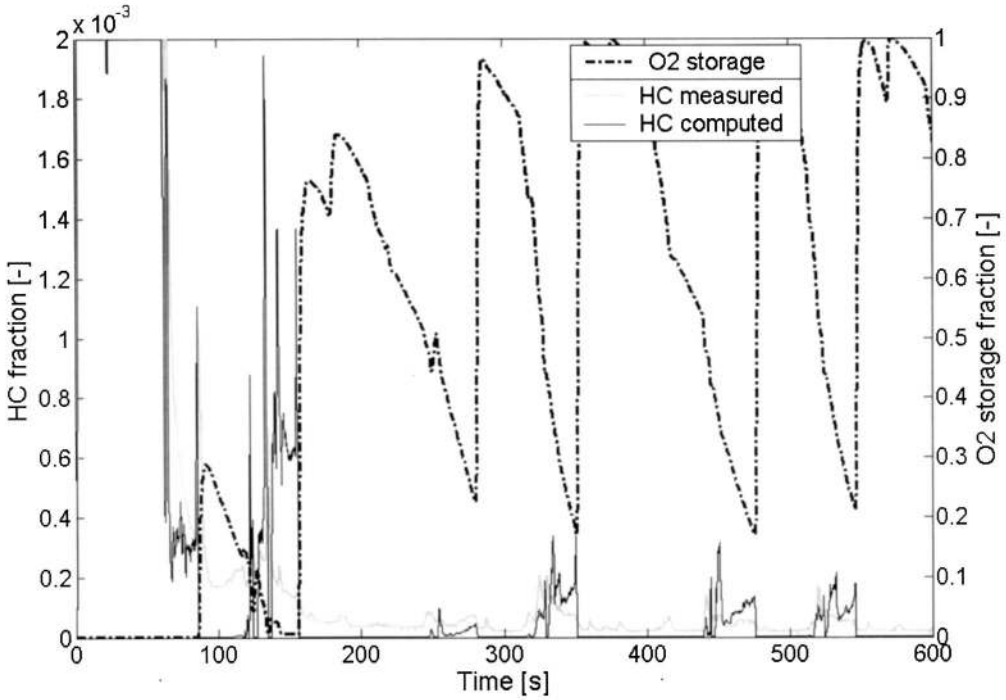

Fig. 9 Computed and measured instantaneous HC emissions at converter inlet and exit during the first 600 sec of NEDC: 2-l-engined passenger car equipped with a 2.4-l underfloor converter with 50-g/ft^3 Pt:Rh catalyst

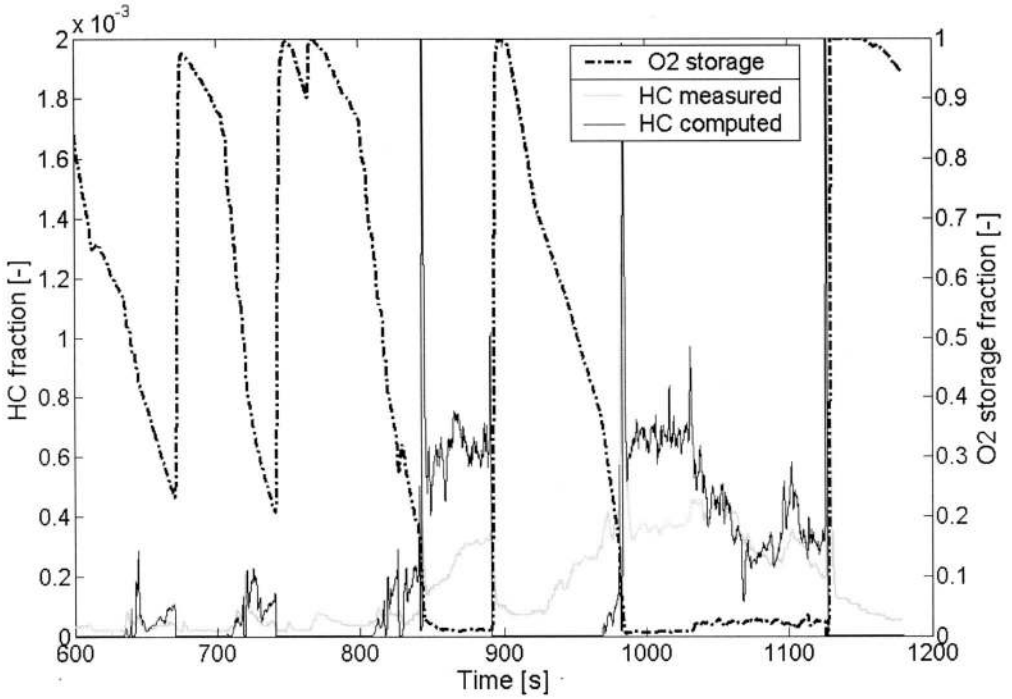

Fig. 10 Computed and measured instantaneous HC emissions at converter inlet and exit during the second half of NEDC: 2-l-engined passenger car equipped with a 2.4-l underfloor converter with 50-g/ft^3 Pt:Rh catalyst

12). Here, the model demonstrates the capacity of taking into account the change in total oxygen storage capacity, to accurately predict the effect of size reduction. The same good behavior is demonstrated with CO in Fig. 13, and NO_x (not shown here).

As a next step, we check the model's predictive ability with a different catalyst type, namely, a Pd:Rh 14:1, 150 gr/ft^3, 0.8-l volume converter, which is now fitted in a close-coupled position on a 2.2-l engined car. Again, the converter is a standard 400-cpsi,

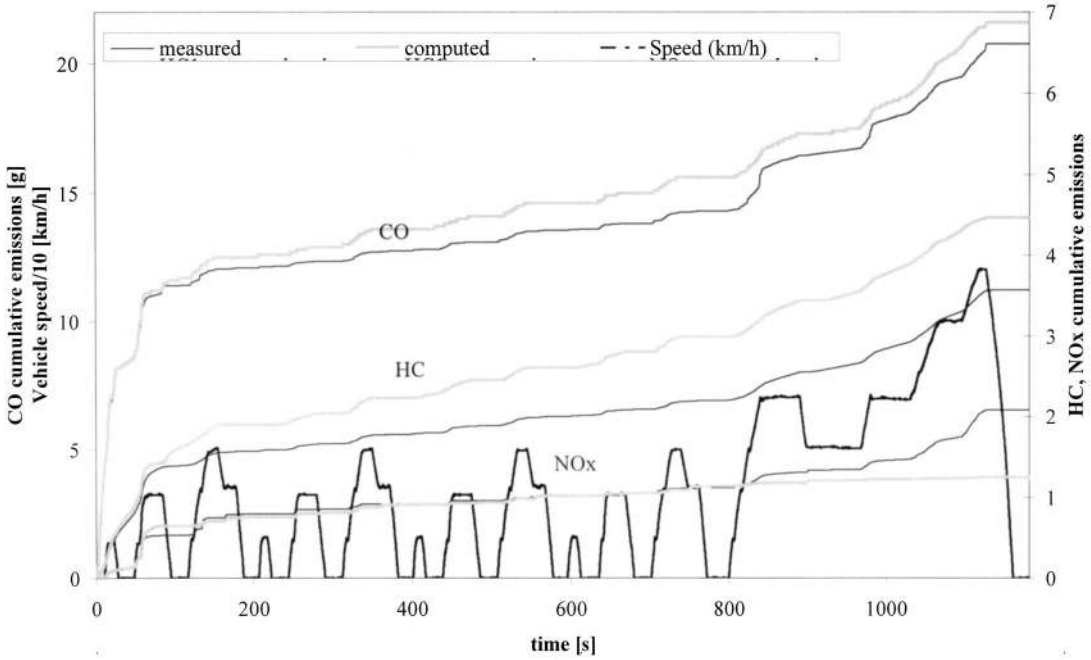

Fig. 11 Computed (based on the kinetics parameters values of Table 1) and measured cumulative CO, HC, and NO_x emissions at converter exit during NEDC. 2-l-engined passenger car equipped with a 0.6-l underfloor converter with 50-g/ft^3 Pt:Rh catalyst. Apparently, the model is capable of predicting the significant difference in CO, HC, and NO_x emissions at the exit of the reduced-size converter.

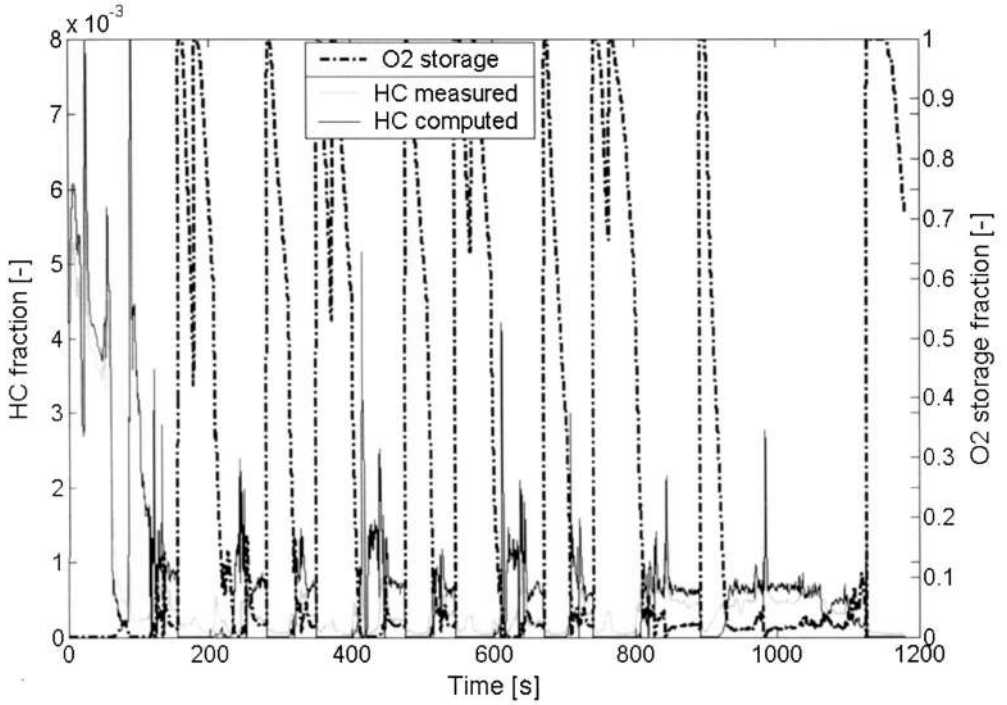

Fig. 12 Computed (based on the kinetics parameters values of Table 1) and measured instantaneous HC emissions at converter exit during NEDC: 2-l-engined passenger car equipped with a 0.6-l underfloor converter with 50-g/ft^3 Pt:Rh catalyst. Apparently, the model is capable of predicting with good accuracy the characteristic HC breakthrough with the reduced-size converter during the high-speed part of NEDC.

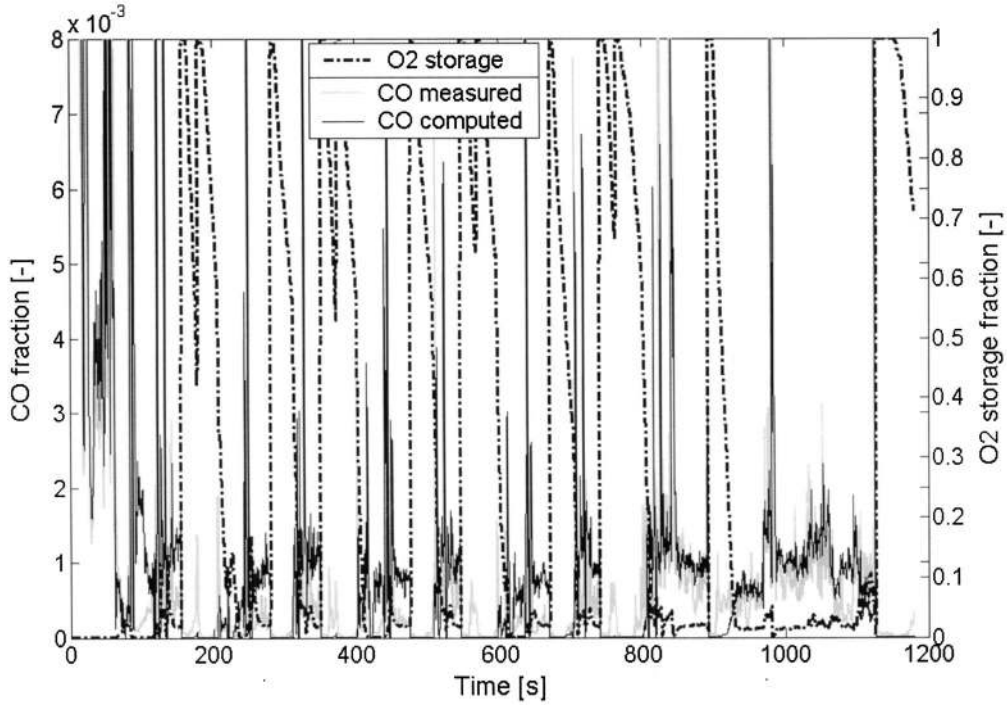

Fig. 13 Computed (based on the kinetics parameters values of Table 1) and measured instantaneous CO emissions at converter exit during NEDC: 2-l-engined passenger car equipped with a 0.6-l underfloor converter with 50-g/ft^3 Pt:Rh catalyst

Table 4 Kinetics parameters tuned to the Pd:Rh catalyst

	Reaction	*A*	*E*
1	$CO+1/2O_2 \rightarrow CO_2$	1.10*E*+18	90,000
2	$H_2+1/2O_2 \rightarrow H_2O$	1.10*E*+18	90,000
3, 4	$C_\alpha H_\beta+(\alpha+0.25\beta)O_2 \rightarrow \alpha CO_2+0.5\beta H_2O$	2.00*E*+15	70,000
		1.00*E*+16	105,000
	NO reduction		
5	$2CO+2NO \rightarrow 2CO_2+N_2$	1.20*E*+13	90,000
	Oxygen storage		
6	$2CeO_2+CO \rightarrow Ce_2O_3+CO_2$	1.00*E*+09	85,000
7, 8	$C_\alpha H_\beta+(2\alpha+\beta)CeO_2 \rightarrow$	7.00*E*+09	85,000
	$\rightarrow(\alpha+0.5\beta)Ce_2O_3+\alpha CO+0.5\beta H_2O$	7.00*E*+09	85,000
9	$Ce_2O_3+1/2O_2 \rightarrow 2CeO_2$	1.00*E*+11	90,000
10	$Ce_2O_3+NO \rightarrow 2CeO_2+1/2N_2$	2.00*E*+11	90,000

6.5-mil substrate. The test now is according to the U.S. FTP-75 procedure, which is considered as a more demanding test procedure for modeling catalytic converter behavior, because of the extensively transient nature of its driving cycle.

In this case, a new kinetic tuning is required, because we shift to a different type of catalyst and washcoat formulation. The genetic algorithm optimized the kinetic parameters of the model for the reference period of the first 600 s of the FTP cycle. This part boldly corresponds to the cold-start phase of the cycle. (This phase is followed by the transient phase (505–1369 s) and the hot-start phase (1369–1874 s), the latter starting after the engine is stopped for 10 min). The values of the kinetic parameters resulting from the tuning procedure are listed in Table 4.

The computed results are summarized in the form of cumulative CO, HC, and NO_x emissions at the catalyst's exit, compared to the corresponding measured curves in Fig. 14. The performance measure takes the value of $F'=0.955$. In addition, computed and measured temperatures at converter's exit are compared in Fig. 15. Apparently, also in this case, the model is capable of matching the catalyst's behavior with very good accuracy, allowing the performance of design optimization studies.

The model's accuracy can be assessed in more detail, by means of instantaneous emissions comparison. As an example, Fig. 16 presents the computed and measured instantaneous HC emissions at converter inlet and exit during the first 600 sec of FTP-75: Apparently, the model successfully matches light-off behavior of the catalyst, as well as subsequent breakthrough during the significant accelerations of FTP cycle. Again, the role of oxygen storage and release reactions in matching the HC breakthrough behavior is very well assessed by including in the graph, the computed degree of filling of the total washcoat's oxygen storage capacity.

The above indicative results can be considered to support a clear demonstration of the attainable accuracy and predictive ability of this category of models. Of course, these results have been achieved by continuous development and improvements of the specific model based on its extensive application in standard exhaust aftertreatment system design case studies during the last six years.

Moreover, the demonstrated model's capacity to predict the combined effect of the precious metal and Ceria kinetics on the transient converter's performance, allows us to support the complex optimization tasks of great interest to the emissions control engineer [45]. For example, a specific catalyst-washcoat design needs to be tailored to address specific converter's performance requirements, based on the raw emissions, exhaust temperature levels, and exhaust mass flowrate behavior of each different type of engine-vehicle-exhaust system combination.

Concluding Remarks

This paper aims to contribute towards a more clear definition of the state of the art in engineering design tools in automotive catalytic converter systems.

A model developed and continuously improved in the authors' lab, based on the experience from involvement in engineering design tasks during the last six years, is described in detail, in its current status of development, in comparison with other models existing in the literature, and employed in demonstration case studies with Pt:Rh and Pd:Rh catalysts.

A kinetic parameter estimation methodology that has been recently developed specifically to support this type of modeling is

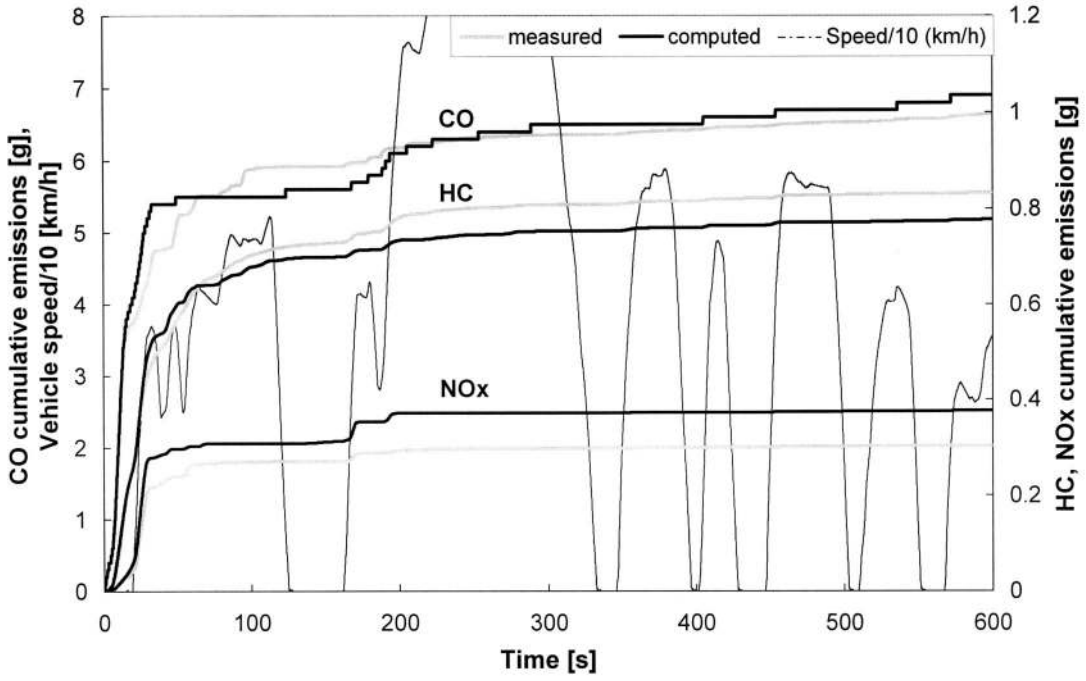

Fig. 14 Computed and measured cumulative CO, HC, and NO_x emissions at converter exit during FTP-75: 2.2-l-engined passenger car equipped with a 0.8-l close-coupled converter with 150-g/ft^3 Pd:Rh catalyst

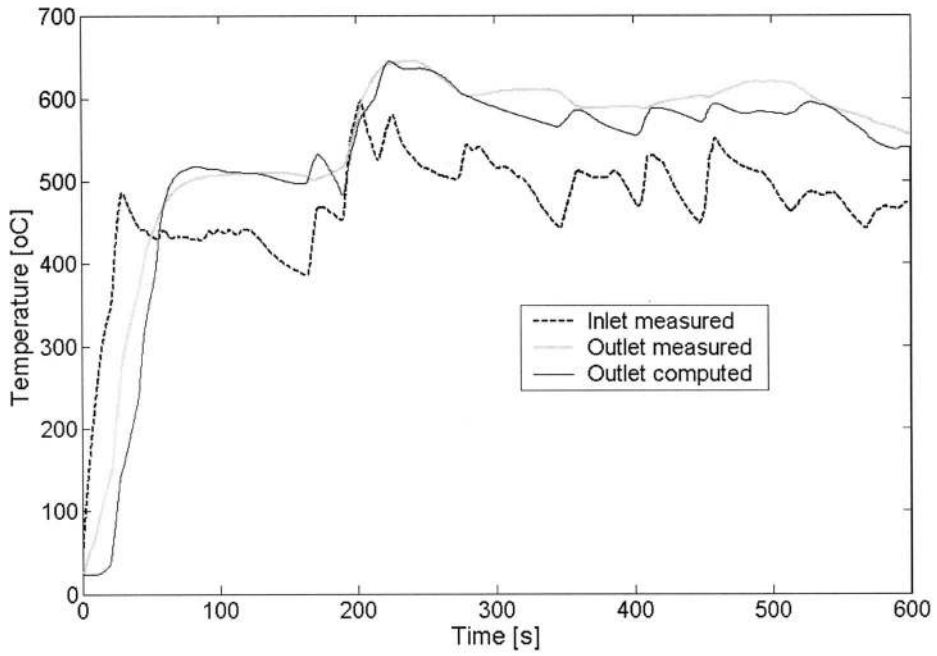

Fig. 15 Computed and measured converter exit temperatures during the first 600 sec of FTP-75 test cycle: 2.2-l-engined passenger car equipped with a 0.8-l close-coupled converter with 150-g/ft^3 Pd:Rh catalyst. Converter inlet temperature recording is also shown.

briefly presented and demonstrated in the case studies. This methodology is based on a combination of a genetic algorithm approach and a customized performance measure. The methodology proves quite successful in finding the parameters for the best fit of the model to the tuning data.

The model's predictions are compared to the respective experimental results, to enable an objective assessment of attainable accuracy. The comparison of measurements and computations is made in terms of cumulative CO, HC, and NO_x emissions at the converter exit, exhaust temperatures at the converter exit, as well

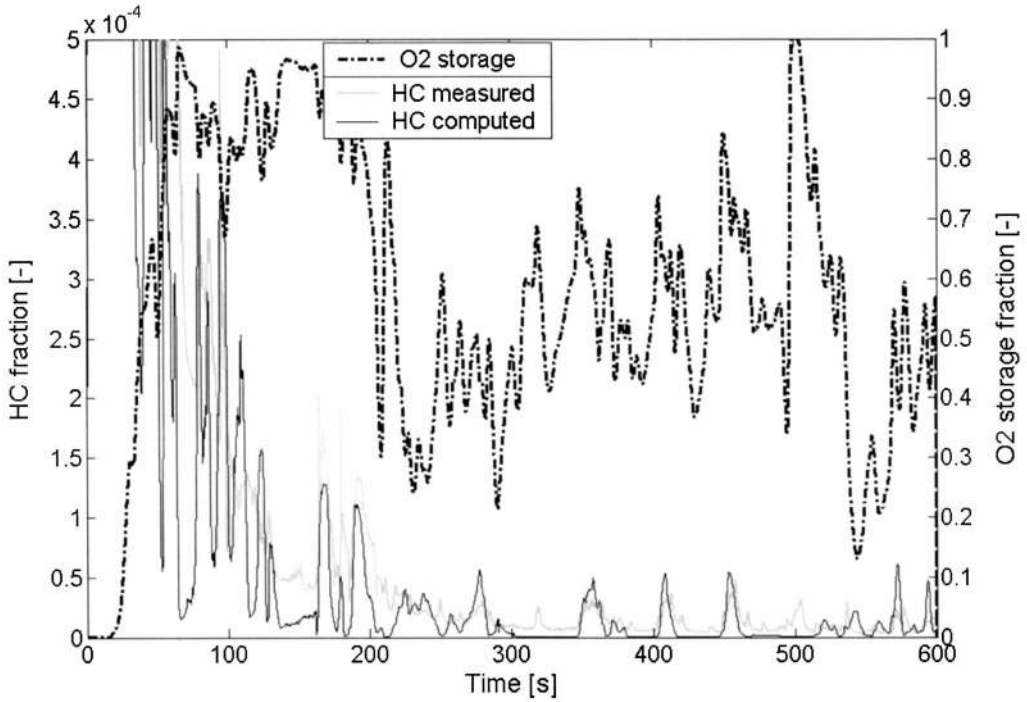

Fig. 16 Computed and measured instantaneous HC emissions at converter exit during the first 600 sec of FTP-75 test cycle: 2.2-l-engined passenger car equipped with a 0.8-l close-coupled converter with 150-g/ft^3 Pd:Rh catalyst

as instantaneous CO, HC, and NO_x emissions at the converter's exit, the latter being the most demanding task for a model.

In order to better quantify model accuracy in matching the experimental results, for the purpose of driving the genetic algorithm towards better solutions, a performance measure is developed and discussed in this paper. This performance measure, in addition to being essential in the parameter estimation methodology, may prove useful to assess the success of modeling exercises by this and other models of catalytic converters.

The overall demonstration is intended to show that the current state-of-the-art models of automotive catalytic converters provide an indispensable tool assisting the design of catalytic exhaust aftertreatment systems for ultra low emitting vehicles. This is succeeded due to the high accuracy attained by such models, despite their simplified kinetics scheme and their engineering approach with minimized degrees of freedom.

Nomenclature

$a_{j,k}$ = Stoichiometric coefficient of species j in reaction k
A = Pre-exponential factor of reaction rate expression (mol K/(m^3 s)
c = Species concentration (−)
c_p = Specific-heat capacity (J/(kg K))
e = Error between computeration and experiment (−)
E = i Activation energy of reaction rate expression (J)
ii Conversion efficiency (−)
f = Performance function (−)
F = Performance measure (−)
G = Inhibition term (Table 1) (K)
ΔH = Molar heat of reaction (J/mol)
h = Convection coefficient (W/(m^2 s))
k = Thermal conductivity (W/(m K))
k_m = Mass transfer coefficient (m/s)
K = Inhibition term (Table 1) (−)
ℓ = Genetic algorithm binary encoding resolution (−)
$\dot{m}$ = Exhaust gas mass flow rate (kg/s)
M = Molecular mass (kg/mol)
N_R = Number of reactions (−)
N_P = Number of tunable parameters (−)
Q_{amb} = Heat trasferred between converter and ambient air (J/(m^3 s))
r = Rate of reaction (mol/m^3 s)
R_g = Universal gas constant (8.314 J/(mol K))
$\dot{R}$ = Rate of species production/depletion per unit reactor volume (mol/(m^3 s))
S = Geometric surface area per unit reactor volume (m^2/m^3)
t = Time (s)
T = Temperature (K)
u_z = Exhaust gas velocity (m/s)
z = Distance from the monolith inlet (m)

Greek Letters

α = Number of carbon atoms in hydrocarbon molecule (−)
β = Number of hydrogen atoms in hydrocarbon molecule (−)
γ = Catalytic surface area per unit washcoat volume (m^2/m^3)
δ = Washcoat thickness (m)
ε = Emissivity factor (radiation) (−)
ϑ = Tunable parameters vector
ρ = Density (kg/m^3)
σ = Stefan–Boltzmann constant (W/(m^2 T^4))
τ = Reference time period for parameter estimation (s)
ψ = Fractional extent of the oxygen storage component (−)
Ψ_{cap} = Washcoat capacity of the oxygen storage component (mol/m^3)

Subscripts

amb = Ambient
g = Gas
i = Parameter index
j = Species index
k = Reaction index
mon = Monolith
n = Time index
in = Inlet
s = (i) Solid; (ii) solid–gas interface
z = Axial direction

References

[1] Farrauto, R. J., and Heck, R. M., 1999, "Catalytic Converters: State of the Art and Perspectives," Catal. Today, **51**, pp. 351–360.
[2] Koltsakis, G. C., and Stamatelos, A. M., 1997, "Catalytic Automotive Exhaust Aftertreatment," Prog. Energy Combust. Sci., **23**, pp. 1–37.
[3] Oh, S. H., and Cavendish, J. C., 1982, "Transients of Monolithic Catalytic Converters: Response to Step Changes in Feedstream Temperature as Related to Controlling Automobile Emissions," Ind. Eng. Chem. Prod. Res. Dev., **21**, pp. 29–37.
[4] Oh, S. H., and Cavendish, J. C., 1985, "Mathematical Modeling of Catalytic Converter Light-off—Part II: Model Verification by Engine-Dynamometer Experiments," AIChE J., **31**(6), pp. 935–942.
[5] Oh, S. H., and Cavendish, J. C., 1985, "Mathematical Modeling of Catalytic Converter Light-off—Part III: Prediction of Vehicle Exhaust Emissions and Parametric Analysis," AIChE J., **31**(6), pp. 943–949.
[6] Tischer, S., Correa, C., and Deutshmann, O., 2001, "Transient Three-Dimensional Simulation of a Catalytic Combustion Monolith Using Detailed Models for Heterogeneous and Homogeneous Reactions and Transport Phenomena," Catal. Today, **69**, pp. 57–62.
[7] Pontikakis, G., and Stamatelos, A., 2001, "Mathematical Modeling of Catalytic Exhaust Systems for EURO-3 and EURO-4 Emissions Standards," Proc. Inst. Mech. Eng., Part D (J. Automob. Eng.), **215**, pp. 1005–1015.
[8] Young, L. C., and Finlayson, B. A., 1976, "Mathematical Models of the Monolithic Catalytic Converter: Part I. Development of Model and Application of Orthogonal Collocation," AIChE J., **22**(2), pp. 331–343.
[9] Siemund, S., Leclerc, J. P., Schweich, D., Prigent, M., and Castagna, F., 1996, "Three-Way Monolithic Converter: Simulations Versus Experiments," Chem. Eng. Sci., **51**(15), pp. 3709–3720.
[10] Koltsakis, G. C., Konstantinidis, P. A., and Stamatelos, A. M., 1997, "Development and Application Range of Mathematical Models for Automotive 3-Way Catalytic Converters," Appl. Catal., B, **12**(2-3), pp. 161–191.
[11] Chen, D. K. S., Bisset, E. J., Oh, S. H., and Van Ostrom, D. L., 1988, "A Three-Dimensional Model for the Analysis of Transient Thermal and Conversion Characteristics of Monolithic Catalytic Converters," SAE paper 880282.
[12] Montreuil, C. N., Williams, S. C., and Adamczyk, A. A., 1992, "Modeling Current Generation Catalytic Converters: Laboratory Experiments and Kinetic Parameter Optimization—Steady State Kinetics," SAE paper 920096.
[13] Dubien, C., Schweich, D., Mabilon, G., Martin, B., and Prigent, M., 1998, "Three-Way Catalytic Converter Modeling: Fast and Slow Oxidizing Hydrocarbons, Inhibiting Species and Steam-Reforming Reaction," Chem. Eng. Sci., **53**(3), pp. 471–481.
[14] Heck, R. H., Wei, J., and Katzer, J. R., 1976, "Mathematical Modeling of Monolithic Catalysts," AIChE J., **22**(3), pp. 477–484.
[15] Shamim, T., Shen, H., Sengupta, S., Son, S., and Adamczyk, A. A., 2002, "A Comprehensive Model to Predict Three-Way Catalytic Converter Performance," J. Eng. Gas Turbines Power, **124**(2), pp. 421–428.
[16] Konstantinidis, P. A., Koltsakis, G. C., and Stamatelos, A. M., 1997, "Computer-Aided Assessment and Optimization of Catalyst Fast Light-off Techniques," Proc. Inst. Mech. Eng., Part D (J. Automob. Eng.), **211**, pp. 21–37.
[17] Konstantinidis, P. A., Koltsakis, G. C., and Stamatelos, A. M., 1998, "The Role of CAE in the Design Optimization of Automotive Exhaust Aftertreatment Systems," Proc. Inst. Mech. Eng., Part D (J. Automob. Eng.), **212**, pp. 1–18.
[18] Baba, N., Ohsawa, K., and Sugiura, S., 1996, "Analysis of Transient Thermal and Conversion Characteristics of Catalytic Converters During Warm-up," JSAE Review of Automative Engineering, **17**, pp. 273–279.
[19] Schmidt, J., Waltner, A., Loose, G., Hirschmann, A., Wirth, A., Mueller, W., Van den Tillaart, J. A. A., Mussmann, L., Lindner, D., Gieshoff, J., Umehara, K., Makino, M., Biehn, K. P., and Kunz, A., 1999, "The Impact of High Cell Density Ceramic Substrates and Washcoat Properties on the Catalytic Activity of Three Way Catalysts," SAE paper 1999-01-0272.

[20] Stamatelos, A. M., Koltsakis, G. C., and Kandylas, I. P., 1999, "Computergestützte Entwurf von Abgasnachbehandlungsystemen. Teil I. Ottomotor," Motortech. Z., **MTZ 60**(2), pp. 116–124.
[21] LTTE-University of Thessaly: CATRAN Catalytic Converter Modeling Software, User's Guide, Version v4r2f. Volos, June 2003.
[22] Pontikakis, G. N., and Stamatelos, A. M., 2002, "Catalytic Converter Modeling: Computer-Aided Parameter Estimation by use of Genetic Algorithms" Proc. Inst. Mech. Eng., Part D: J. Automob. Eng., accepted for publication.
[23] Pontikakis, G., 2003, "Modeling, Reaction Schemes and Kinetic Parameter Estimation in Automotive Catalytic Converters and Diesel Particulate Filters," Ph.D. thesis, Mechanical & Industrial Engineering Department, University of Thessaly, June 2003. http://www.mie.uth.gr/labs/ltte/pubs/PhD_G_Pont.pdf
[24] Zygourakis, K., and Aris, R., 1983, "Multiple Oxidation Reactions and Diffusion in the Catalytic Layer of Monolith Reactors," Chem. Eng. Sci., **38**(5), pp. 733–744.
[25] Hoebink, J. H. B. J., van Gemert, R. A., van den Tillaart, J. A. A., and Marin, G. B., 2000, "Competing Reactions in Three-Way Catalytic Converters: Modeling of the NO_x Conversion Maximum in the Light-off Curves Under Net Oxidizing Conditions," Chem. Eng. Sci., **55**(9), pp. 1573–1581.
[26] Keren, I., and Sheintuch, M., 2000, "Modeling and Analysis of Spatiotemporal Oscillatory Patterns During CO Oxidation in the Catalytic Converter," Chem. Eng. Sci., **55**, pp. 1461–1475.
[27] Voltz, S. E., Morgan, C. R., Liederman, D., and Jacob, S. M., 1973, "Kinetic Study of Carbon Monoxide and Propylene Oxidation on Platinum Catalysts," Ind. Eng. Chem. Prod. Res. Dev., **12**, pp. 294–301.
[28] Young, L. C., and Finlayson, B. A., 1976, "Mathematical Models of the Monolithic Catalytic Converter: Part I. Development of Model and Application of Orthogonal Collocation," AIChE J., **22**(2), pp. 337–343.
[29] Hayes, R. E., and Kolaczkowski, S. T., 1994, "Mass and Heat Transfer Effects in Catalytic Monolith Reactors," Chem. Eng. Sci., **46**(21), pp. 3587–3599.
[30] Tanaka, M., Tsujimoto, Y., Miyazaki, T., Warashina, M., and Wakamatsu, S., 2001, "Pecularities of Volatile Hydrocarbons Emissions From Several Types of Vehicles in Japan," Chemosphere-Global Change Science, **3**(2), pp. 185–197.
[31] Pattas, K. N., Stamatelos, A. M., Pistikopoulos, P. K., Koltsakis, G. C., Konstantinidis, P. A., Volpi, E., and Leveroni, E., 1994, "Transient Modeling of 3-Way Catalytic Converters," SAE paper 940934, SAE Trans., **103**, pp. 565–578.
[32] Koberstein, E., and Wannemacher, G., 1987, "The A/F Window With Three-Way Catalysts. Kinetic and Surface Investigations," *CAPOC, International Congress on Catalysis and Automotive Pollution Control*, Brussels.
[33] Siemund, S., Leclerc, J. P., Schweich, D., Prigent, M., and Castagna, F., 1996, "Three Way Monolithic Converter: Simulations Versus Experiments," Chem. Eng. Sci., **51**(15), pp. 3709–3720.
[34] Heck, R. H., Wei, J., and Katzer, J. R., 1976, "Mathematical Modeling of Monolithic Catalysts," AIChE J., **22**(3), pp. 477–484.
[35] Zygourakis, K., 1989, "Transient Operation of Monolith Catalytic Converters: A Two-Dimensional Reactor Model and the Effects of Radially Nonuniform Flow Distributions," Chem. Eng. Sci., **44**, pp. 2075–2086.
[36] Jahn, R., Snita, D., Kubicek, M., and Marek, M., 1997, "3-D Modeling of Monolith Reactors," Catal. Today, **38**, pp. 39–46.
[37] Dubien, C., and Schweich, D., 1997, "Three Way Catalytic Converter Modeling. Numerical Determination of Kinetic Data," in *CAPOC IV, Fourth International Congress on Catalysis and Automotive Pollution Control*, Brussels.
[38] Pontikakis, G. N., Papadimitriou, C., and Stamatelos, A. M., 2004, "Kinetic Parameter Estimation by Standard Optimization Methods in Catalytic Converter Modeling," Chem. Eng. Commun., **91**, pp. 3–29.
[39] Glielmo, L., and Santini, S., 2001, "A Two-Time-Scale Infinite Adsorption Model of Three-Way Catalytic Converters During the Warm-Up Phase," ASME J. Dyn. Syst., Meas., Control, **123**, pp. 62–70.
[40] Bates, D. M., and Watts, D. G., 1988, *Nonlinear Regression Analysis and its Applications*, Wiley, New York.
[41] Luenberger, D. G., 1989, *Linear and Nonlinear Programming*, Second Edition, Addison-Wesley, Reading, MA.
[42] Goldberg, D. E., 1989, *Genetic Algorithms in Search Optimization, and Machine Learning*, Addison-Wesley, Reading, MA.
[43] Emanuel Falkenauer, 1998, *Genetic Algorithms and Grouping Problems*, Wiley, New York.
[44] Konstantas, G., and Stamatelos, A., 2004, "Quality Assurance of Exhaust Emissions Test Data," Proc. Inst. Mech. Eng., Part D: J. Automob. Eng., , **218**, pp. 901–914.
[45] Votsmeier, M., Bog, T., Lindner, D., Gieshoff, J., Lox, E. S., and Kreuzer, T., 2002, "A System(atic) Approach Towards Low Precious Metal Three-Way Catalyst Application," SAE paper 2002-01-0345.